Electronic and structural properties of quaternary compounds

唐毓慧（Yu-Hui Tang）

國立中山大學物理所

指導教授 ： 蔡民雄教授

民國九十四年六月一日

Contents

- Motivation

- Calculation methods

- Electronic properties of $Ba_{1-x}Sr_xTiO_3$ and $Pb_{1-x}Sr_xTiO_3$ alloys

- Electronic and magnetic properties of $La_{1-x}Sr_xMnO_3$ and $La_{1-x}Ca_xMnO_3$

- Electronic structures of wide-band-gap $(SiC)_{1-x}(AlN)_x$ semiconductors

- Conclusion

Motivation

❑ <u>Binary compounds</u> :

   Charge transfer and bonding are very simple.

❑ <u>Ternary compounds</u> :

   Charge transfer and bonding are more complicated. But, their electronic structures are derivable from those of the two constituent binary compounds with some modification.

❑ <u>Quaternary compounds</u> :

   The comple and subtle charge transfer may give rise to an electronic structure different from those predicted directly from constituent binary or ternary compounds.

Use of the first-principles calculation method to understand electronic properties of three kinds of quaternary compounds with complicated charge transfer.
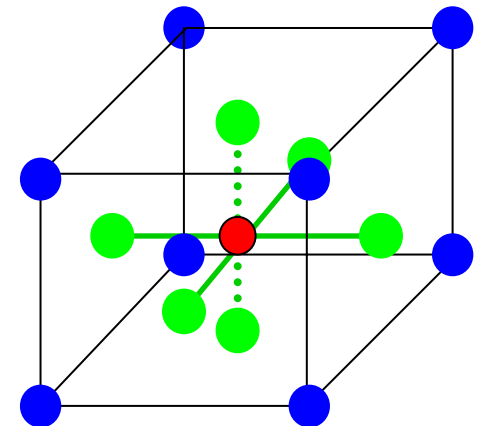
Calculation methods

- First-principles pseudofunction (PSF) calculation method is used to obtain electronic structures.

- First-principles molecular-dynamics (MD) calculation method is used to efficiently obtain the structural parameters.

- These first-principles calculation methods are implemented with the density functional theory (DFT), the local-density approximation (LDA) for paramagnetic calculation, and the local-spin-density approximation (LSDA) for spin-polarized calculation.
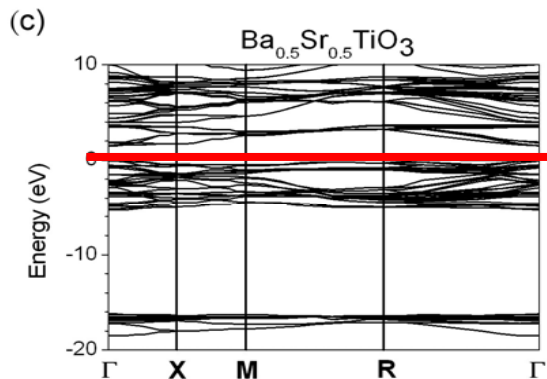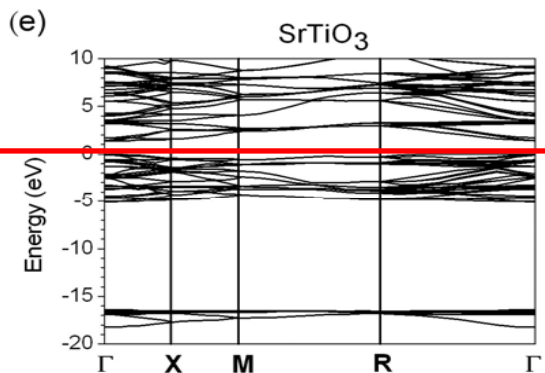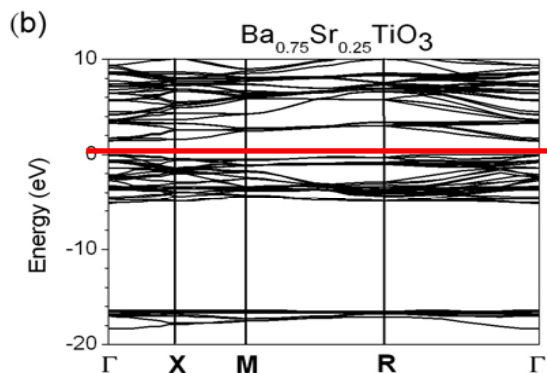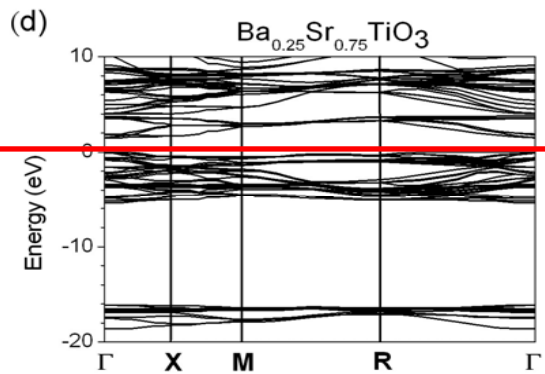
Electronic properties of $Ba_{1-x}Sr_xTiO_3$ (BSTO) and $Pb_{1-x}Sr_xTiO_3$ (PSTO) alloys

- The experimental lattice constant, (a,b,c), of the **perovskite** structure are obtained by the x-ray diffraction (XRD).
- The (2a,2b,c) unit cell and atomic positions of the **undistorted perovskite** structure are used for all cases.

x	c/a (BSTO)	c/a (PSTO)
0.00	1.0074	1.0648
0.25	1.0035	1.0409
0.50	1.0000	1.0000
0.75	1.0000	1.0000
1.00	1.0000	1.0000

The band structures for $Ba_{1-x}Sr_xTiO_3$

(a) $BaTiO_3$

(b) $Ba_{0.75}Sr_{0.25}TiO_3$

(c) $Ba_{0.5}Sr_{0.5}TiO_3$

(d) $Ba_{0.25}Sr_{0.75}TiO_3$

(e) $SrTiO_3$
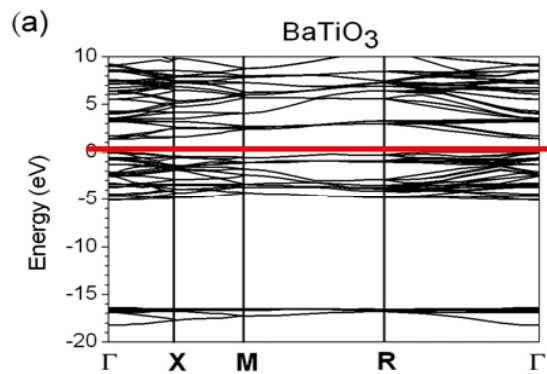
X	Eg(eV)
0.00	1.43 (3.20[1])
0.25	1.46
0.50	1.52
0.75	1.51
1.00	1.49 (3.25[2])

$$\Gamma = (0,0,0) \quad X = \pi\left(\frac{1}{2a},0,0\right) \quad M = \pi\left(\frac{1}{2a},\frac{1}{2b},0\right)$$
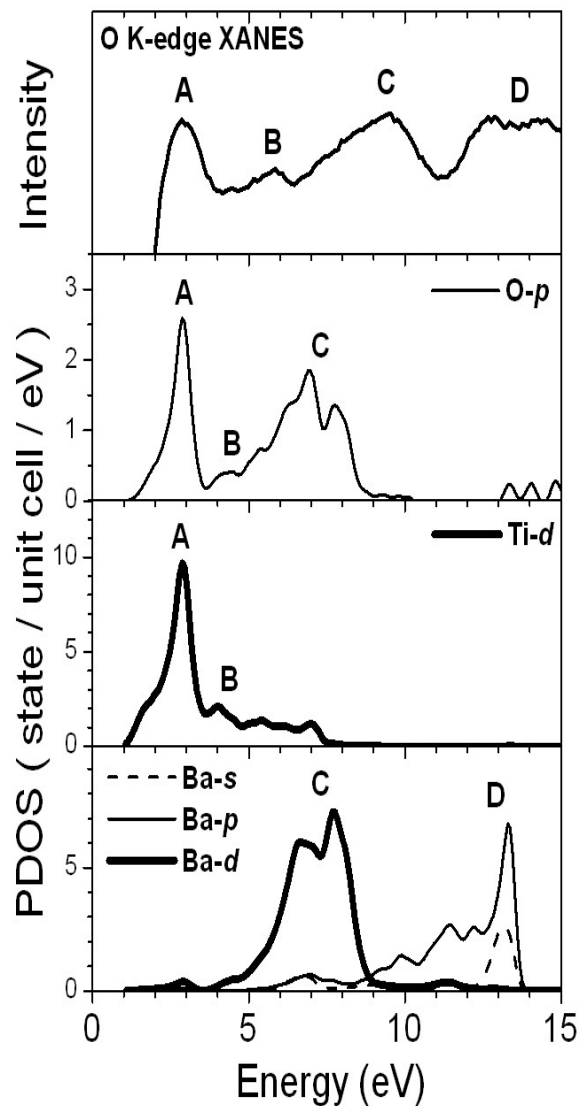
$$R = \pi\left(\frac{1}{2a},\frac{1}{2b},\frac{1}{c}\right)$$

[1] K. Van Benthem et al., J. Appl. Phys. 90, 6156(2001).

[2] S. H. Wemple., Phys. Rev. B2, 2679(1970).

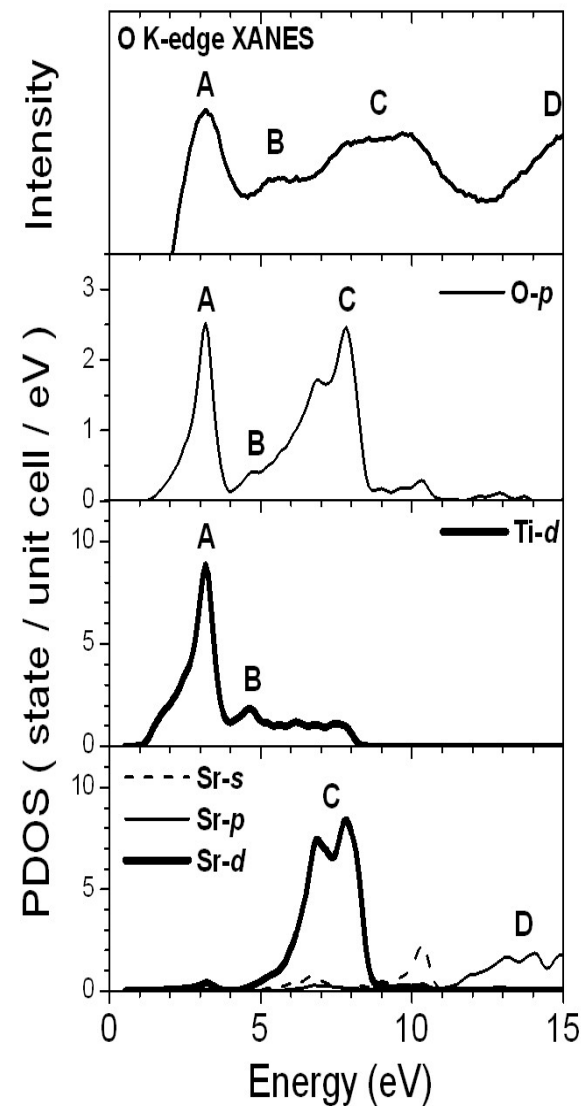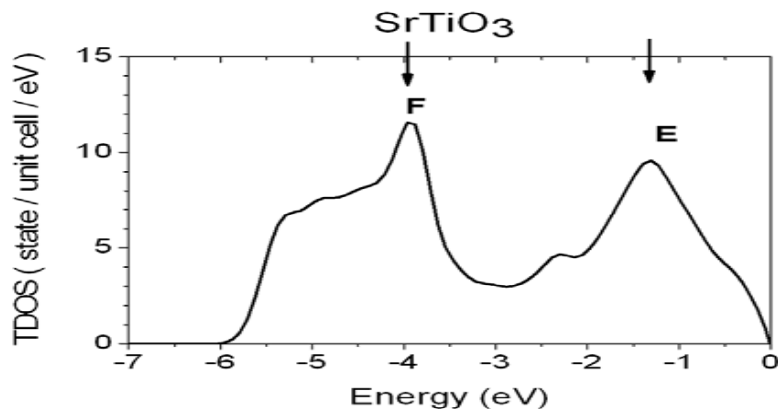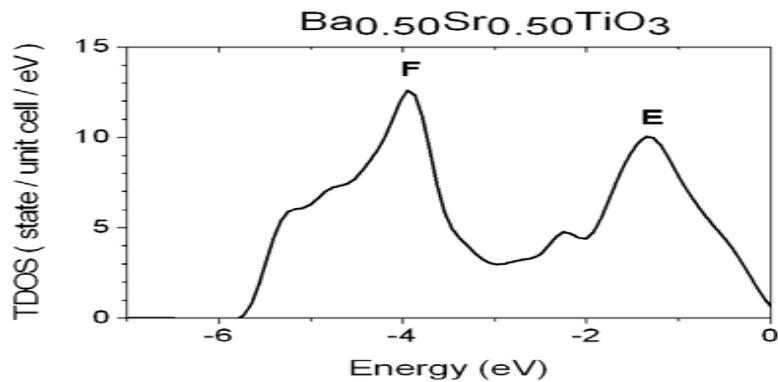# PDOS's and O K-edge XANES spectra of $Ba_{1-x}Sr_xTiO_3$

TDOS's for $Ba_{1-x}Sr_xTiO_3$

BaTiO₃

Ba₀.₅₀Sr₀.₅₀TiO₃

SrTiO₃
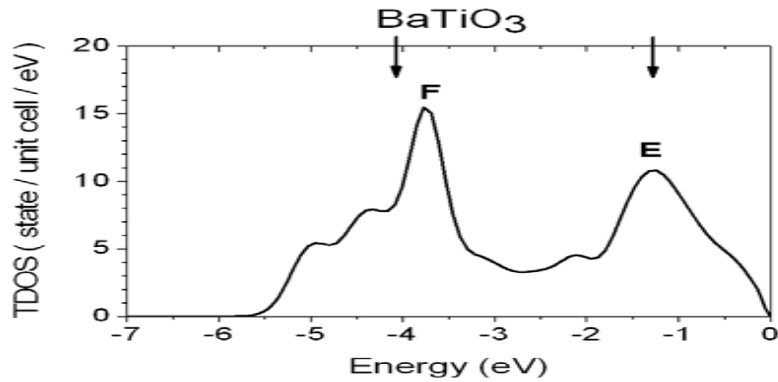
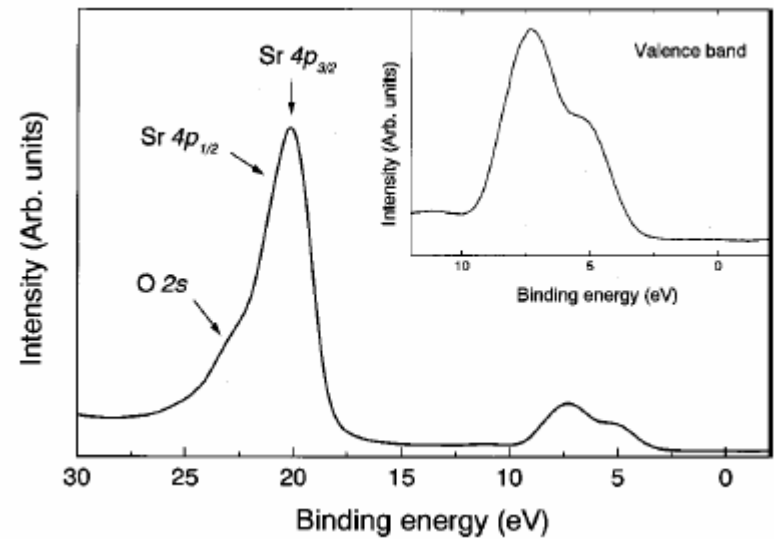| X	Valence bandwidth (eV)
0.00	5.8 (6.0[1])
0.25	5.8
0.50	5.8
0.75	6.0
1.00	6.0 (6.0[2])

E : O-p

F : O-p and Ti-d

[1] P. Pertosa et al., Phys. Rev. **B18**, 5177 (1978).

[2] Shigemi Kohiki et al., Phys. Rev. **B64**, 7964 (2000).

a) UPS
hv = 38 eV

b) LCAO-DOS
(Pertosa et al.
Ref.4)

c) UPS
hv = 105 eV
(Cord et. al
Ref.6)

d) Xα-cluster
calculation for TiO_6
(Tsukada et al.
Ref.24)

Binding Energy (eV)
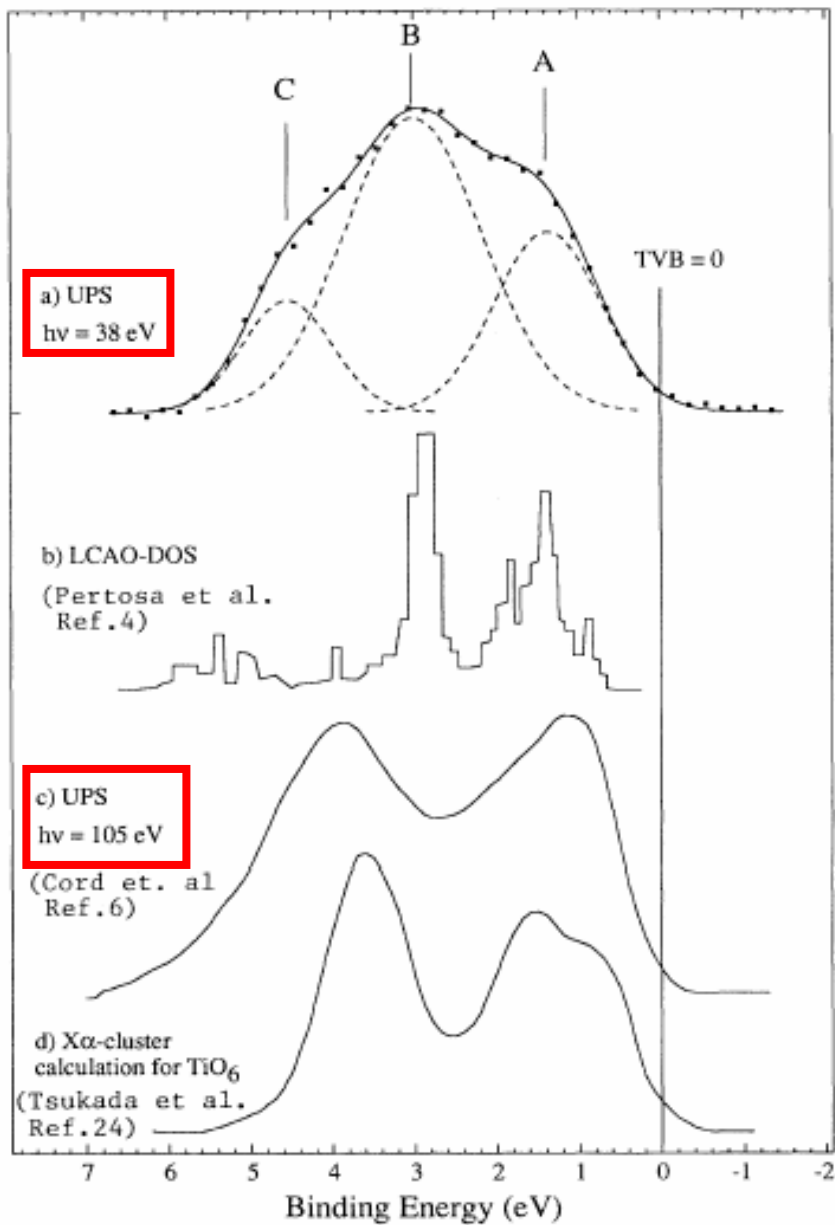
The ultraviolet photoemission (UPS) spectrum for $BaTiO_3$.

The core-level x-ray photoemission spectroscopy (XPS) spectrum for $SrTiO_3$.

The band structures for $Pb_{1-x}Sr_xTiO_3$

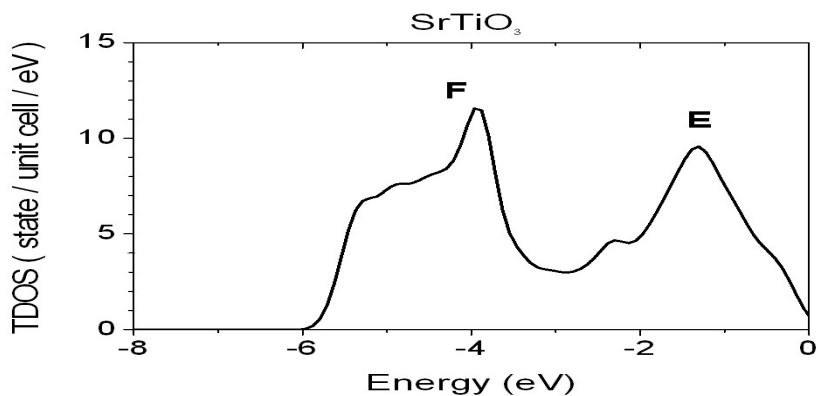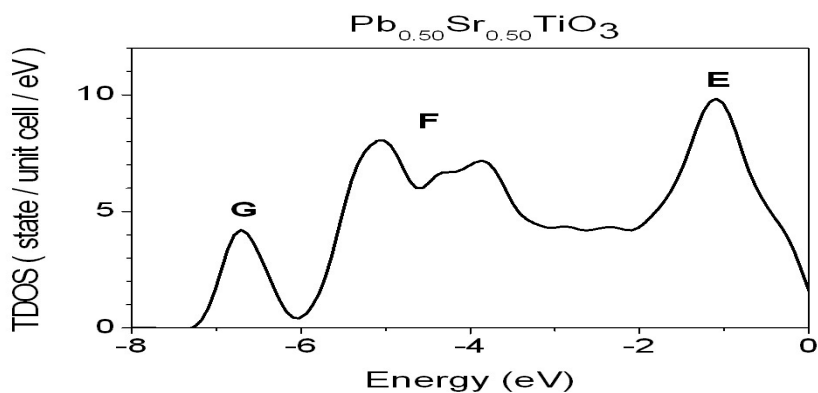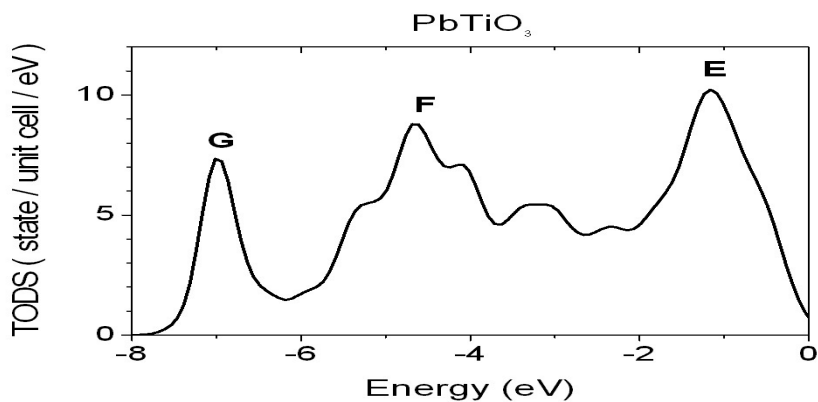(a) $PbTiO_3$

(b) $Pb_{0.75}Sr_{0.25}TiO_3$

(c) $Pb_{0.50}Sr_{0.50}TiO_3$

(d) $Pb_{0.25}Sr_{0.75}TiO_3$
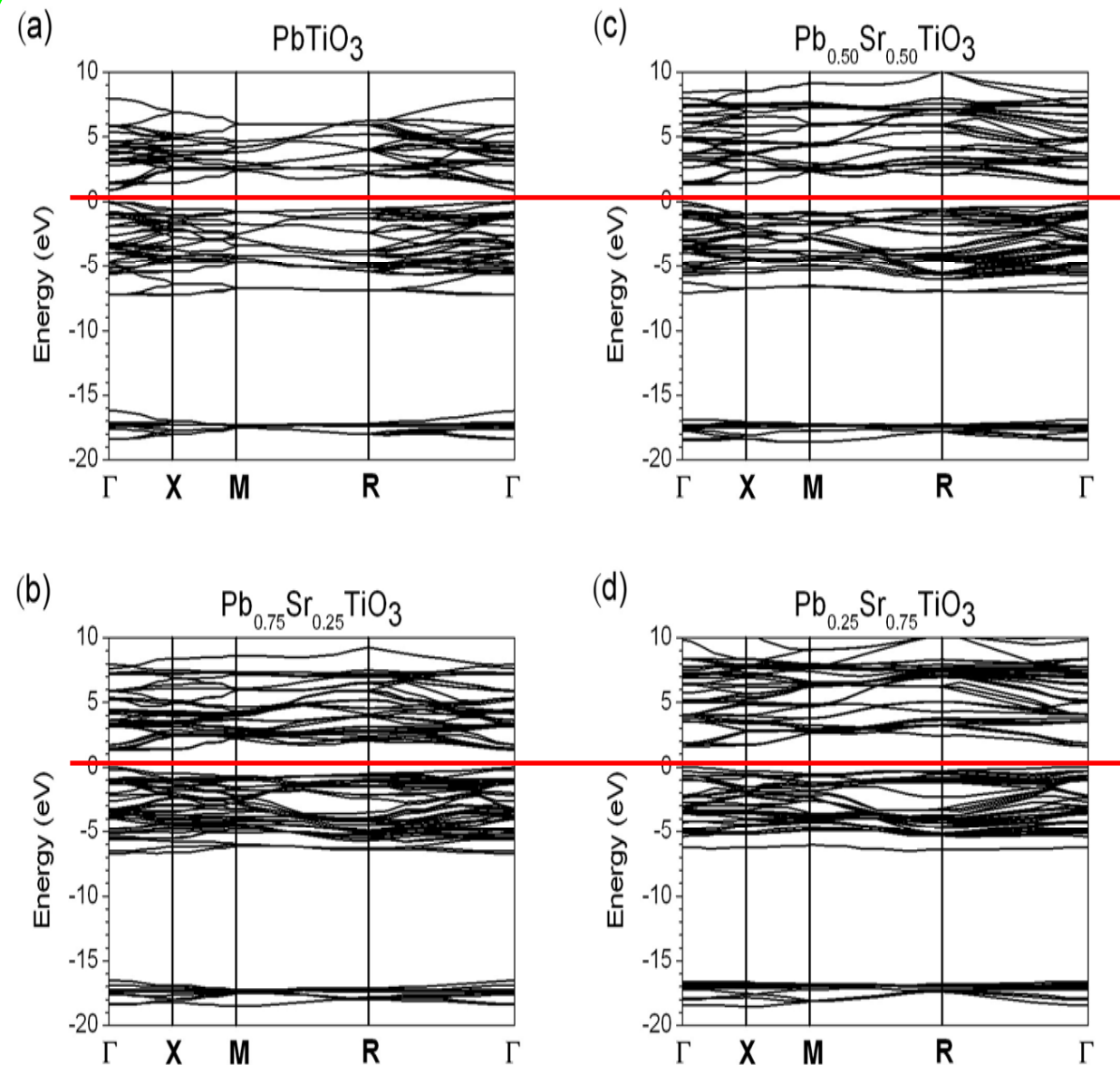
X	Eg(eV)
0.00	0.90
0.25	1.27
0.50	1.35
0.75	1.61
1.00	1.49

More significant variation of band gaps for PSTO than for BSTO.

PDOS's and O *K*-edge XANES spectra for Pb$_{1-x}$Sr$_x$TiO$_3$

TDOS's for $Pb_{1-x}Sr_xTiO_3$

X	Valence bandwidth (eV)
0.00	7.8
0.25	7.4
0.50	7.3
0.75	7.1
1.00	6.0

E : O-*p*   F : O-*p* and Ti-*d*

G : Pb-*s* ➔ enlarge the valance bandwidth

Effective charges for $Ba_{1-x}Sr_xTiO_3$ and $Pb_{1-x}Sr_xTiO_3$
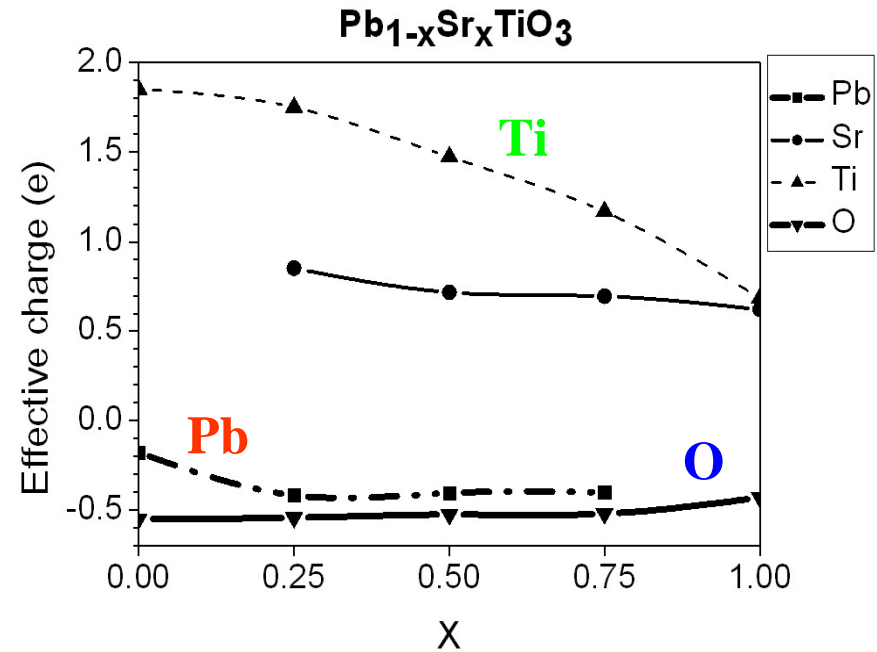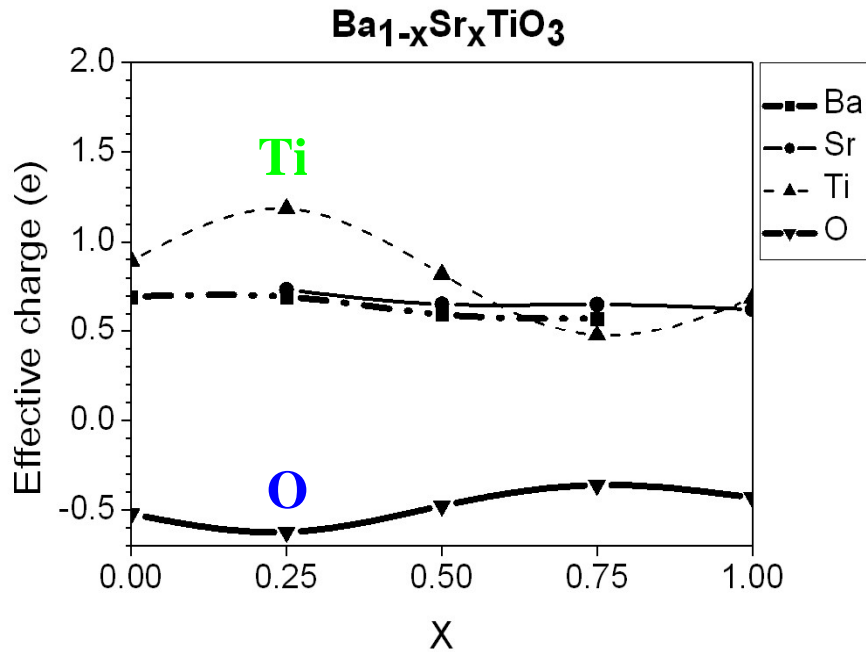
Electronegativity

Ba = 0.89, **Sr** = 0.95, **Ti** = 1.54, **Pb** = 2.33, and **O** = 3.44

Electronic configuration

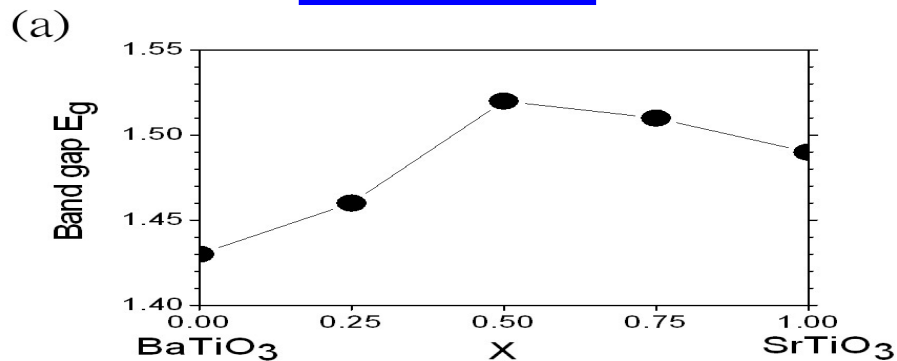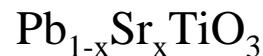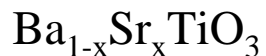**Ba** : $[Xe]6s^2$, **Sr** : $[Ar]5s^2$, **Pb** : $[Xe]6s^2 6p^2$

Extra two *6p* valance electrons of Pb → More repulsive; tends to lose electrons.

Larger electronegativity of Pb→ Tends to gain electrons from Sr and Ti

Variations of band gaps for $Ba_{1-x}Sr_xTiO_3$ and $Pb_{1-x}Sr_xTiO_3$

$Ba_{1-x}Sr_xTiO_3$

$Pb_{1-x}Sr_xTiO_3$
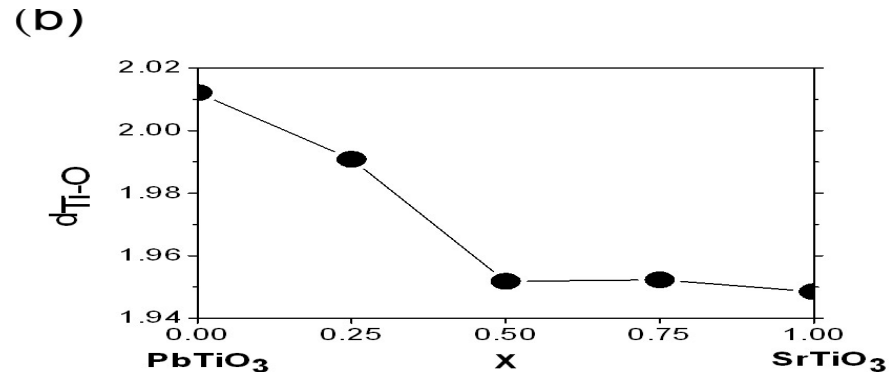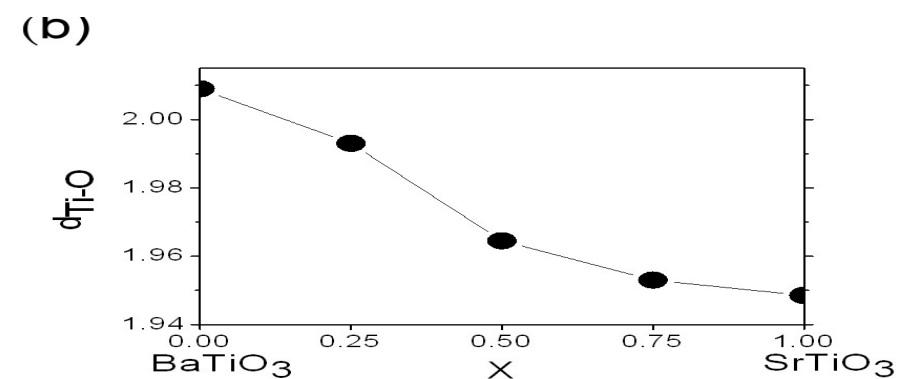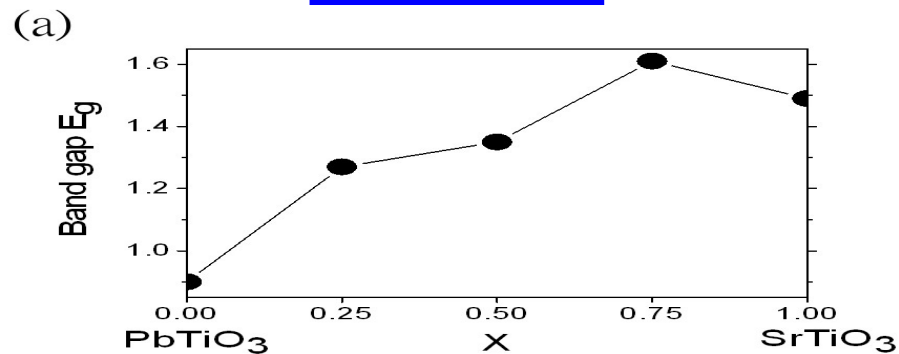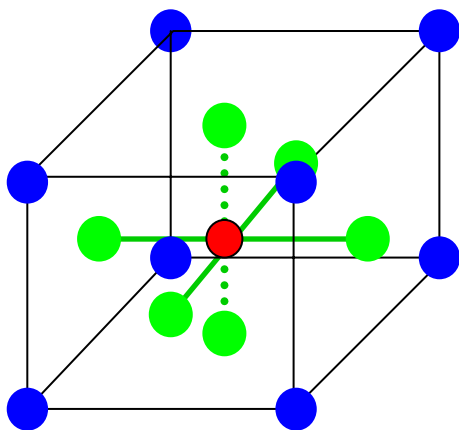

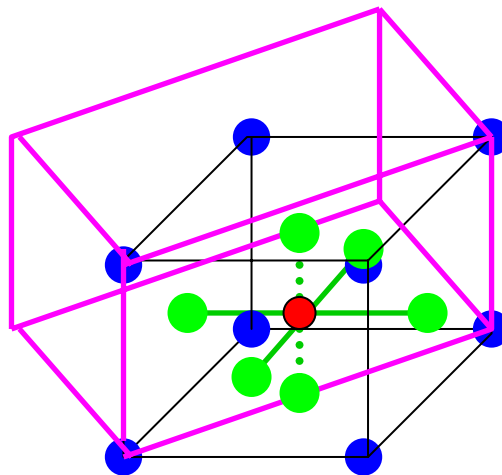Binary compound : cation - anion bond length ⇩   band gap ⬆

(CBM)   (VBM)

BSTO and PSTO : The bowing upward of the calculated band gaps is related

to the bowing downward of the Ti-O bond length.

Electronic and magnetic properties of $La_{1-x}Sr_xMnO_3$ and $La_{1-x}Ca_xMnO_3$

	X	0.00	0.25	0.50	0.75	1.00
X=Ca	Space group	*Pnma*	*Pnma*	*Pnma*	*Pnma*	$Pm\overline{3}m$
X=Sr			$R\overline{3}c$	*Pnma*	*Pnma*	$Pm\overline{3}m$
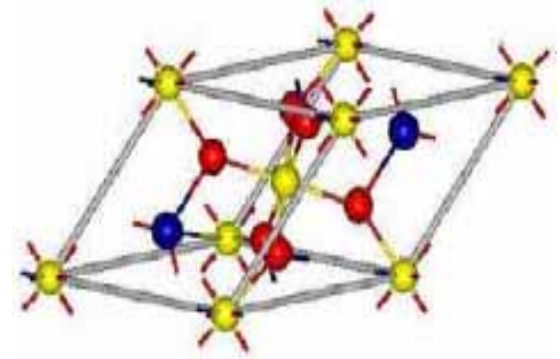
$Pm\overline{3}m$ *Pnma* $R\overline{3}c$

Magnetic states for $La_{1-x}Ca_xMnO_3$ and $La_{1-x}Sr_xMnO_3$

Ca	X=0	X=0.25	X=0.50	X=0.75	X=1
E(F)-E(AF)	0.1375	-0.6625	-0.0025	0.0175	0.0850
Magnetic state	AF	F	F/AF	AF	AF
Sr	X=0	X=0.25	X=0.50	X=0.75	X=1
E(F)-E(AF)	0.1375	-0.3350	-0.0650	0.0475	0.0750
Magnetic state	AF	F	F	AF	AF
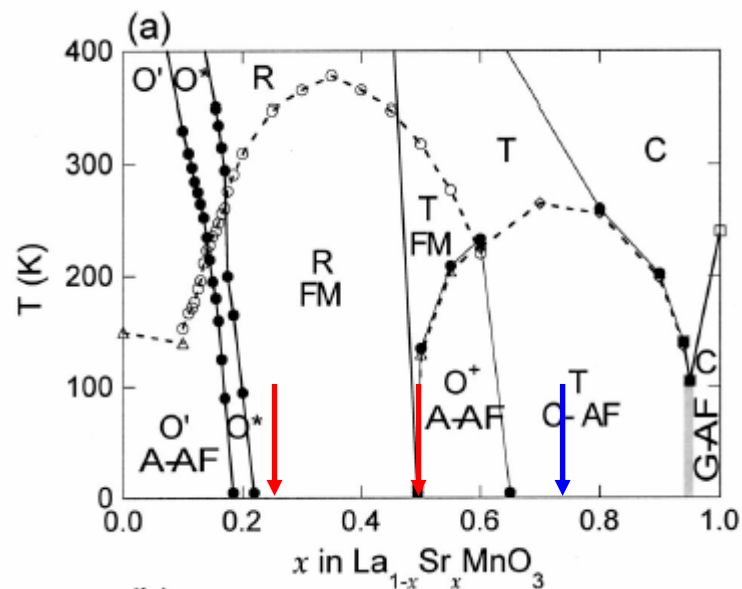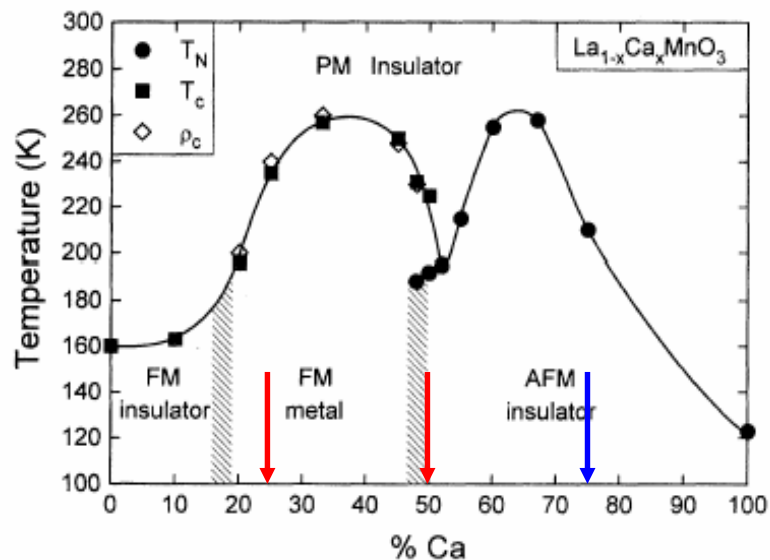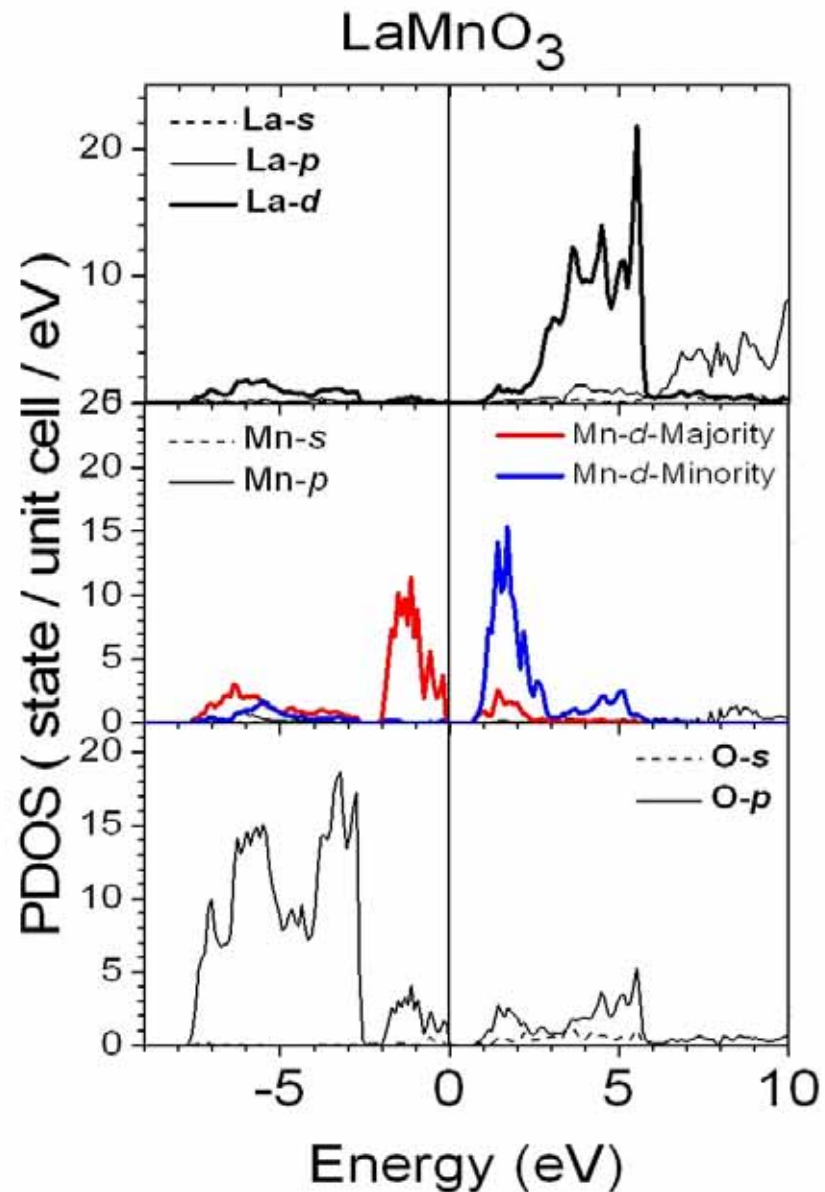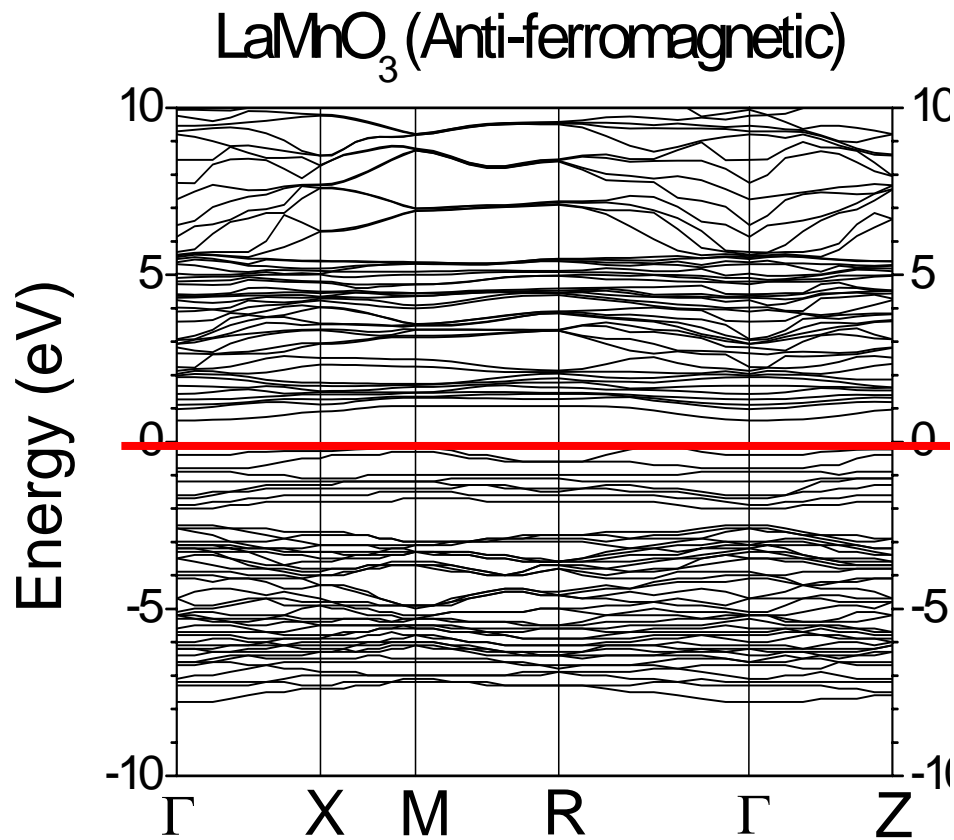
LaMnO$_3$

❑ The calculated band gap for $LaMnO_3$ is about 0.7eV, which is formed between Mn majority-spin e_g and minority-spin t_{2g} sub-bands.
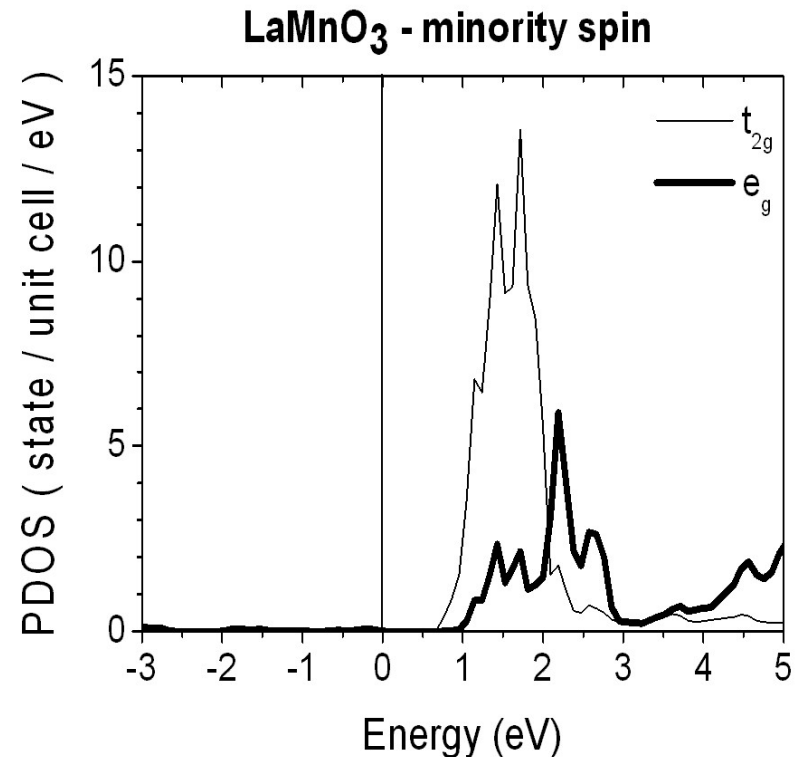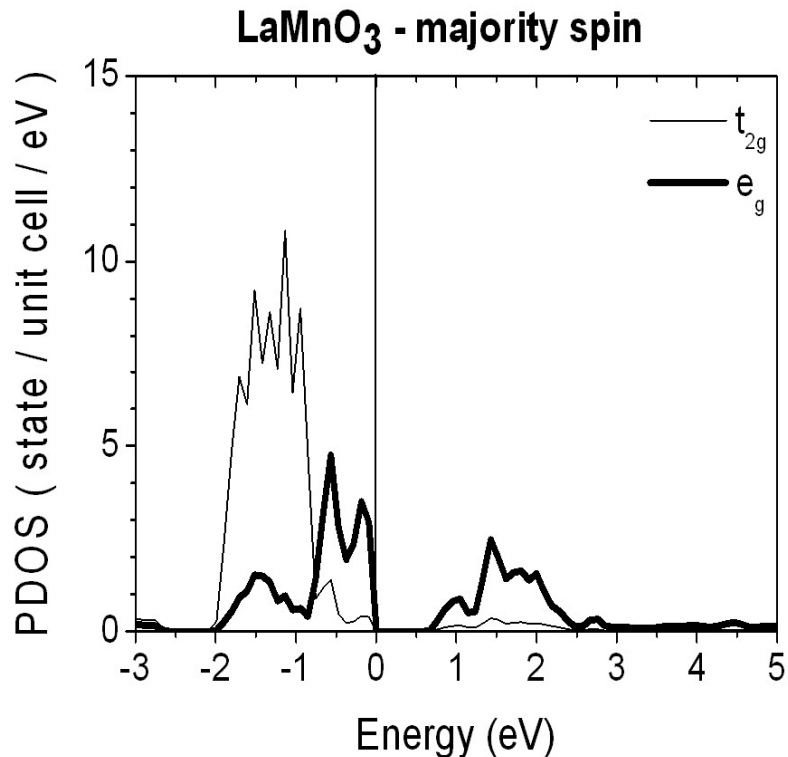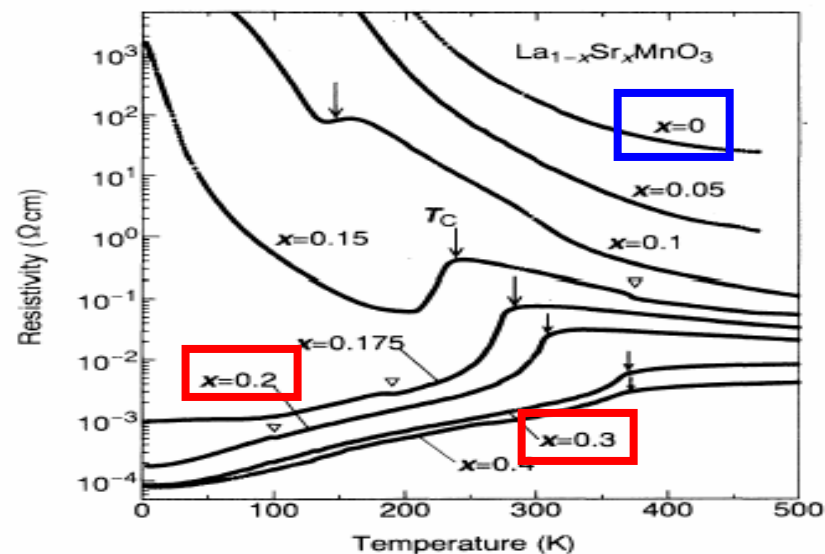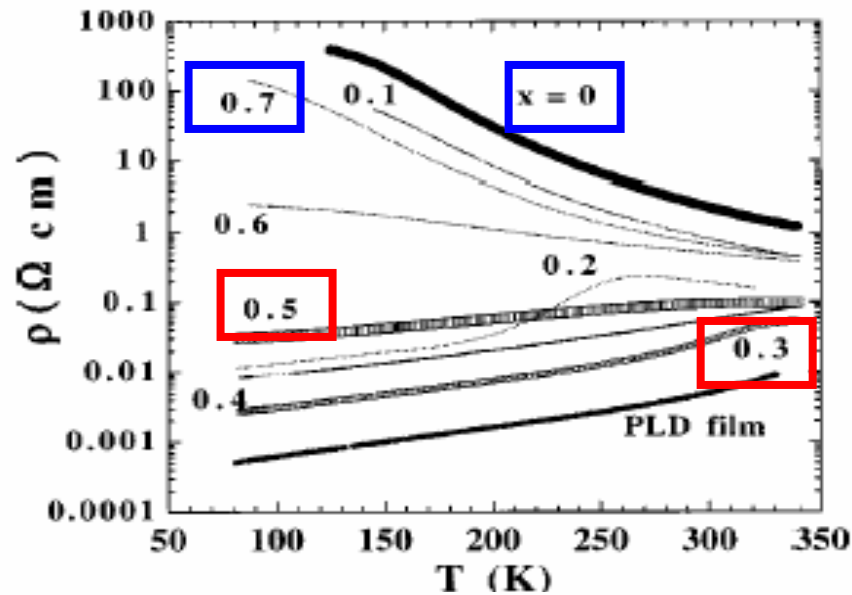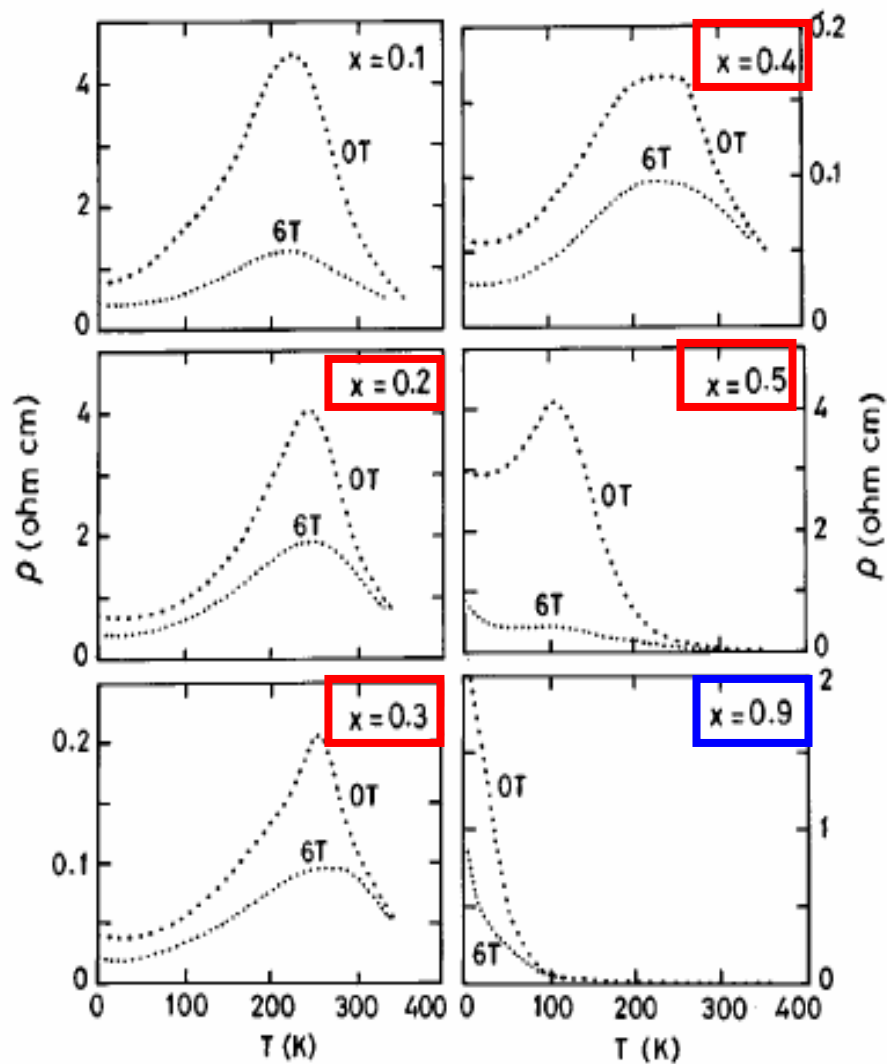
Resistivities of La$_{1-x}$Ca$_x$MnO$_3$ and La$_{1-x}$Sr$_x$MnO$_3$

AF

F

La$_{1-x}$Ca$_x$MnO$_3$

La$_{1-x}$Sr$_x$MnO$_3$

PDOS's of ferromagnetic cases

Delocalized Mn majority-spin e_g

$La_{0.75}Ca_{0.25}MnO_3$
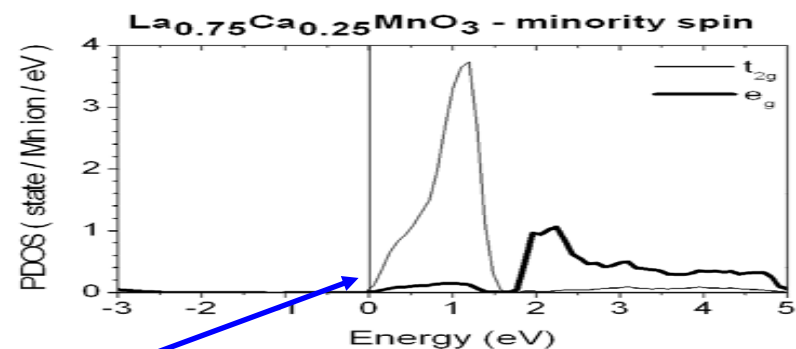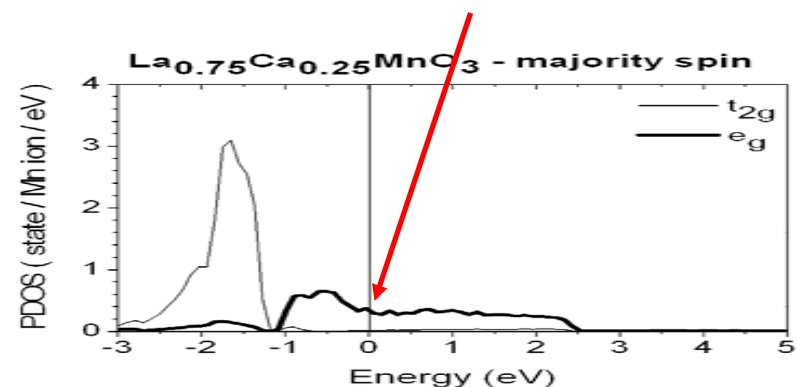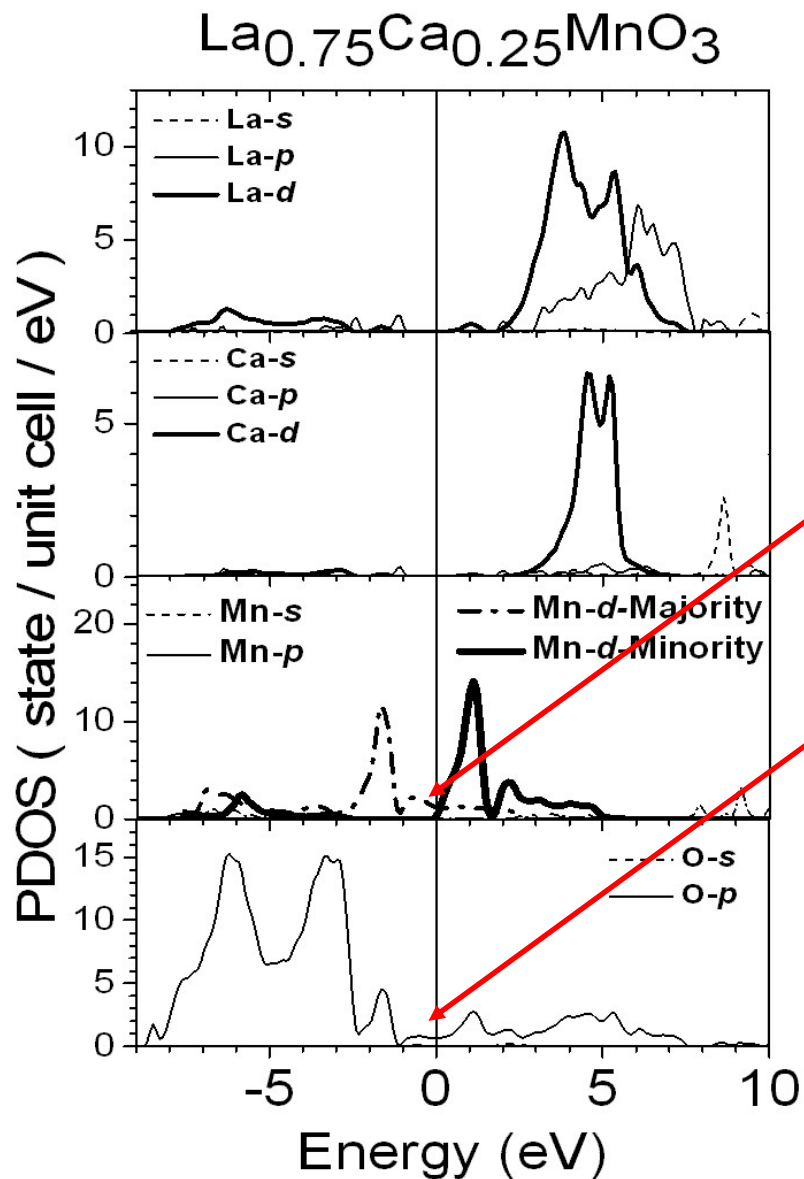
Sharp Mn minority-spin t_{2g}

The observed metal-like behavior is dominantly due to delocalized Mn majority-spin e_g and O-p states.

PDOS's of ferromagnetic cases
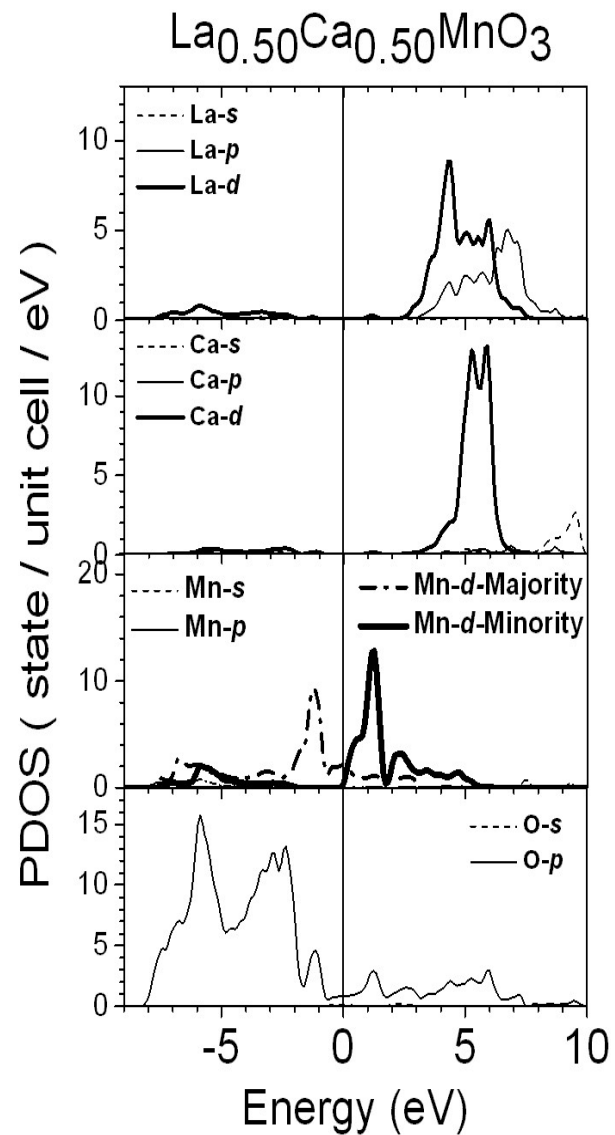
PDOS's of antiferromagnetic cases

La$_{0.25}$Sr$_{0.75}$MnO$_3$

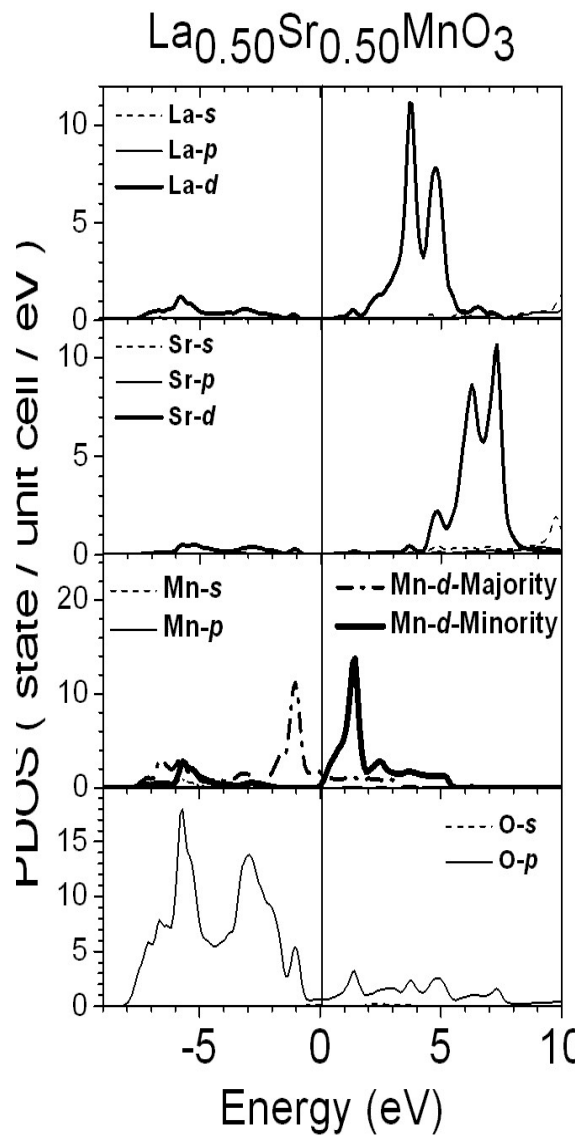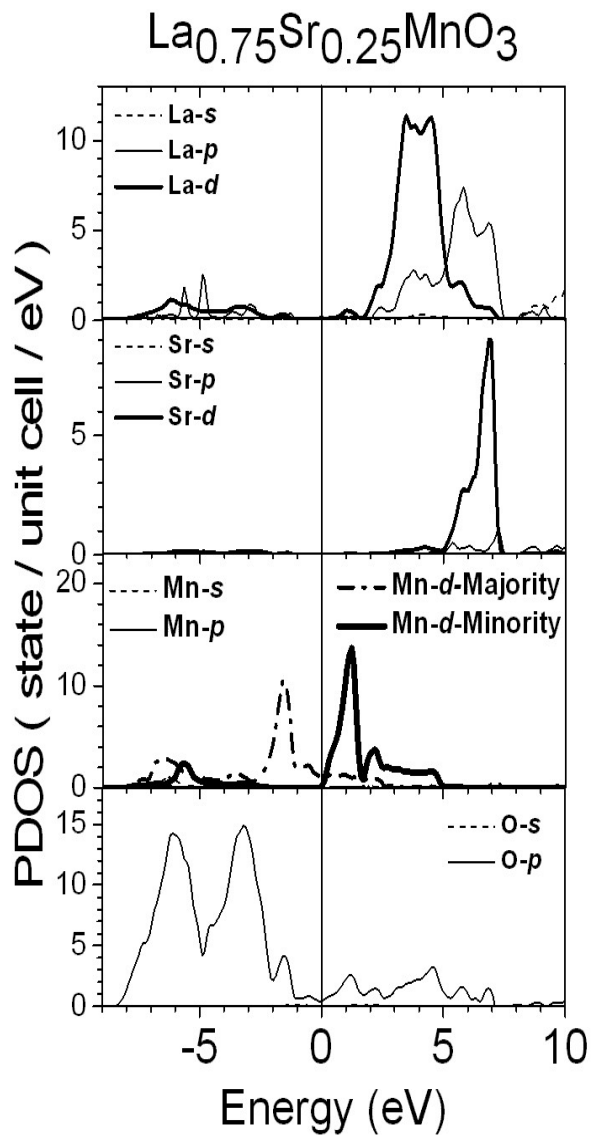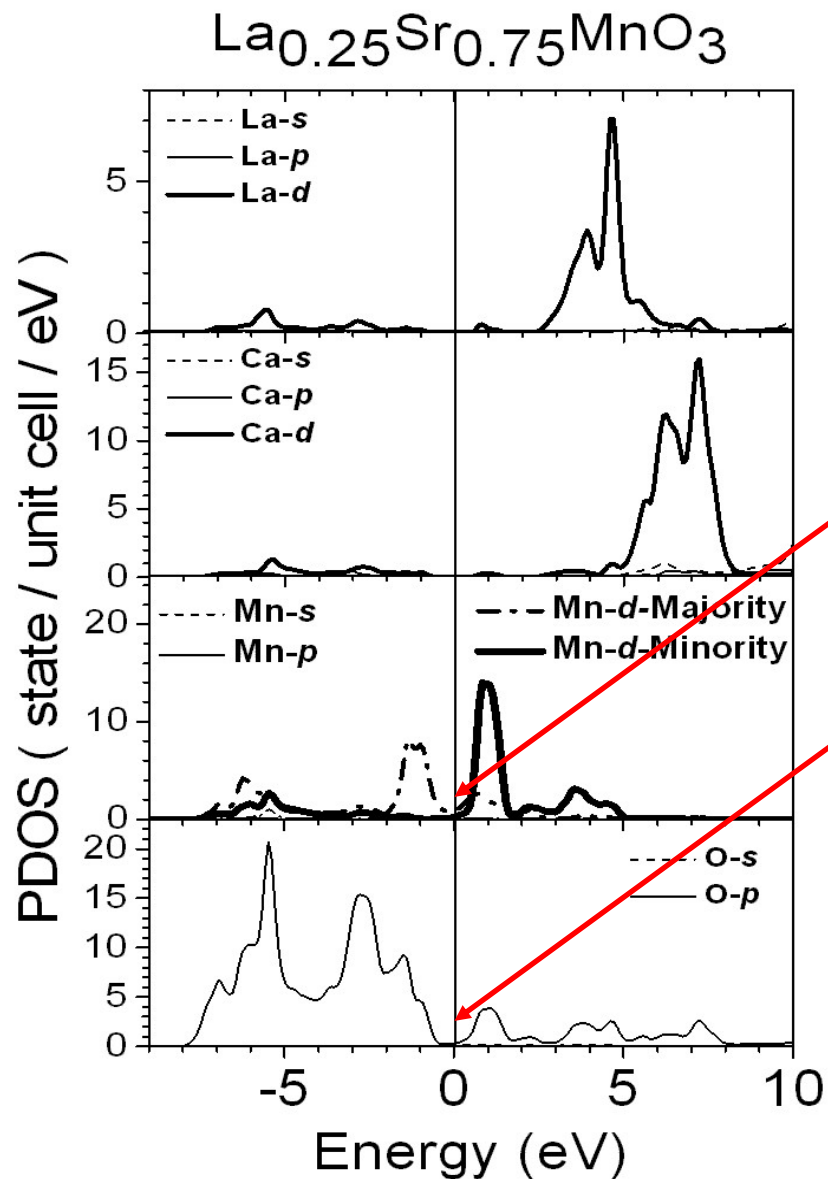Delocalized Mn majority-spin e$_g$

Sharp Mn minority-spin t$_{2g}$
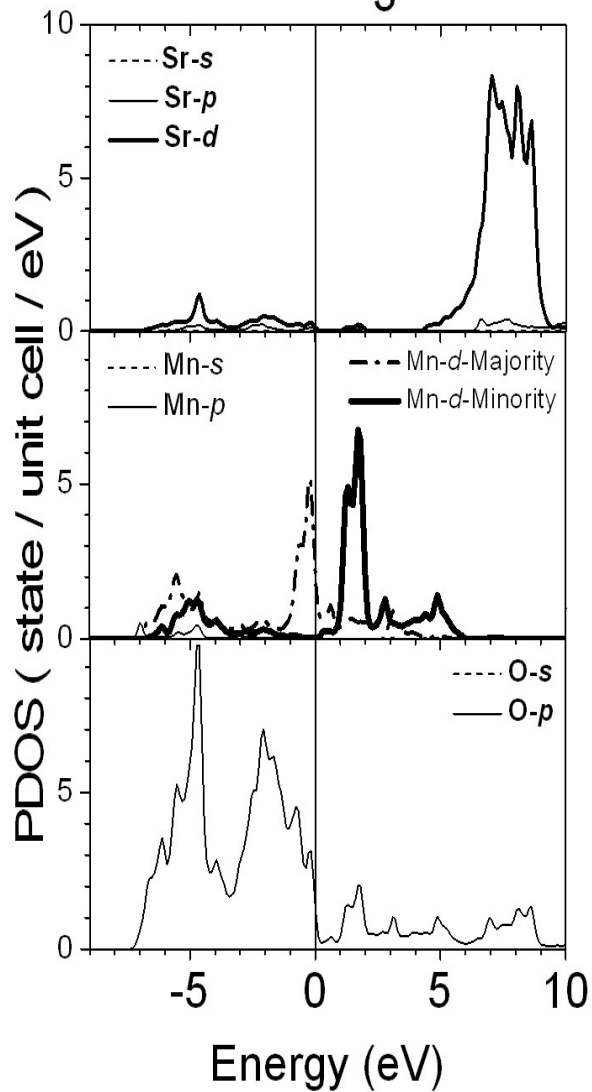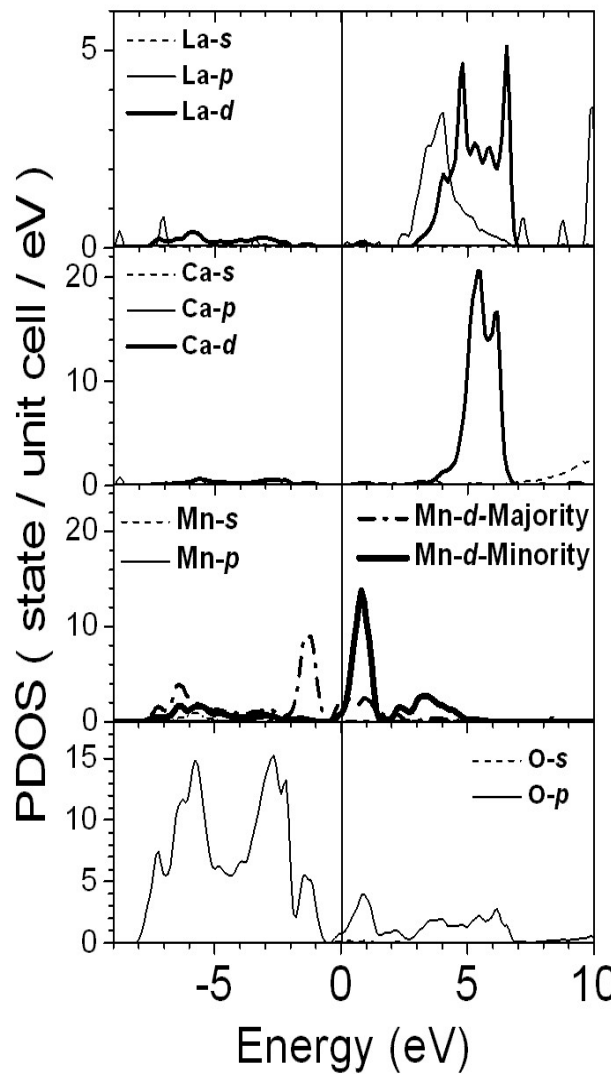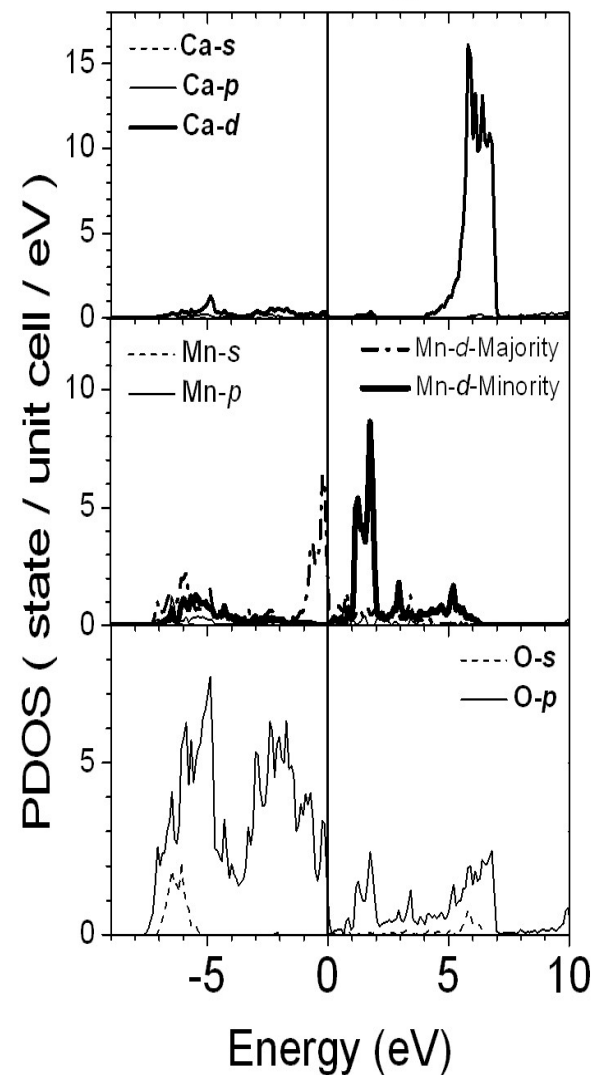
Effective charges for $La_{1-x}Sr_xMnO_3$ and $La_{1-x}Ca_xMnO_3$

(a)

(b)
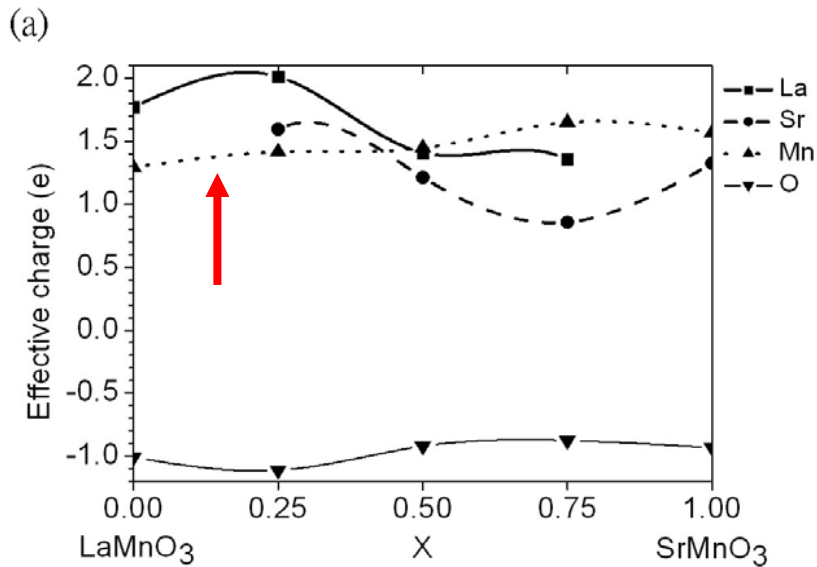
Electronegativity

Sr = 0.95

Ca = 1.00

La = 1.10

Mn = 1.55

O = 3.44
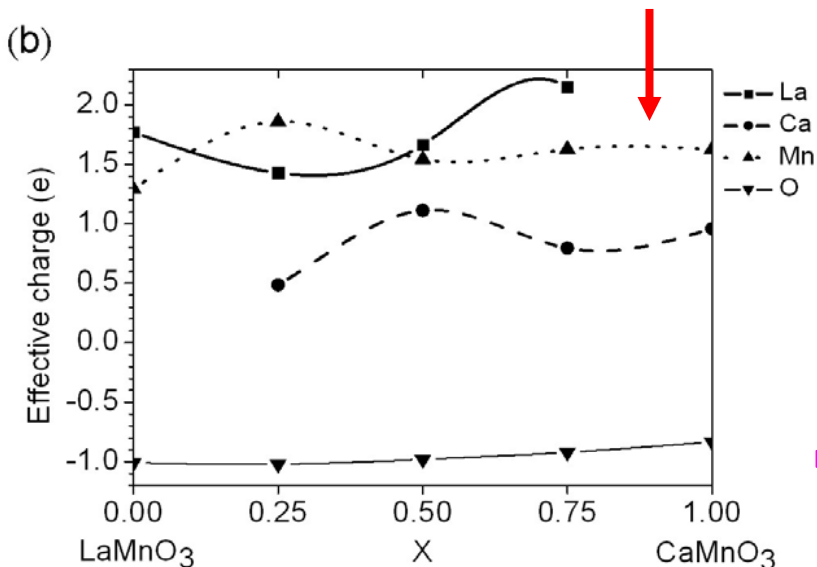
❑ Significant charge transfer is also found in these quaternary compounds.

❑ Effective charge of Mn is **not integer**

Mixed valence picture in doped manganites is questionable.

Questions about the mixed valence picture of Mn ions in hole-doped LaMnO$_3$

❑ The Mn-O bond has a covalent part and is not 100% ionic. Mn and O ions don't have integral effective charges in manganites.

❑ The mixed valence system has a larger electrostatic energy than the uniform valence system.

❑ The on-site Coulomb potentials at Mn^{3+} and Mn^{4+} differ by about $\dfrac{e^2}{\varepsilon \cdot r} = \dfrac{14.4\,eV}{\varepsilon \cdot r\,(\text{Å})}$. This chemical shift is absent in the Mn $3d$ t_{2g} and e_g features in Mn K- and $L_{3,2}$-edge x-ray absorption spectroscopy (XAS) spectra . [1,2]

[1] T. Saitoh et al., Phys. Rev. B51, 13942(1995).
[2] M. Croft et al., Phys. Rev. B48, 8726(1997).

Comparison of the electrostatic energies

Assume **uniform** charge distribution,

Electrostatic energy :

$$u = \frac{z^2 e^2}{\varepsilon r_{Mn}} f(\eta) \quad , \quad \eta = \frac{r_{Mn}}{R}$$
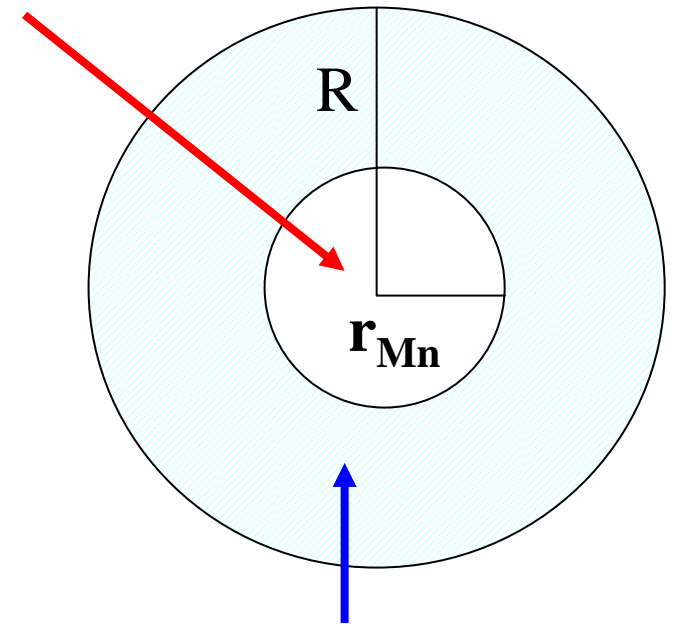
$$f(\eta) = \frac{1}{10}\left[1 + (5 - 9\eta + 5\eta^3 - \eta^6)/(1-\eta^3)^2\right]$$

~ 0.6 for small

1) Mn^{3+} and Mn^{4+} : $u_1 = \dfrac{180\,eV}{\varepsilon}$

2) $Mn^{3.5+}$ and $Mn^{3.5+}$: $u_2 = \dfrac{176\,eV}{\varepsilon}$

** The difference is larger for real charge distributions

Positive Mn ion with effective charge Ze

R

r_{Mn}

Negative compensating charge

Origin of the magnetism in $La_{1-x}Sr_xMnO_3$ and $La_{1-x}Ca_xTiO_3$

□ Splitting of majority- and minority-spin sub-bands due to the exchange interaction.
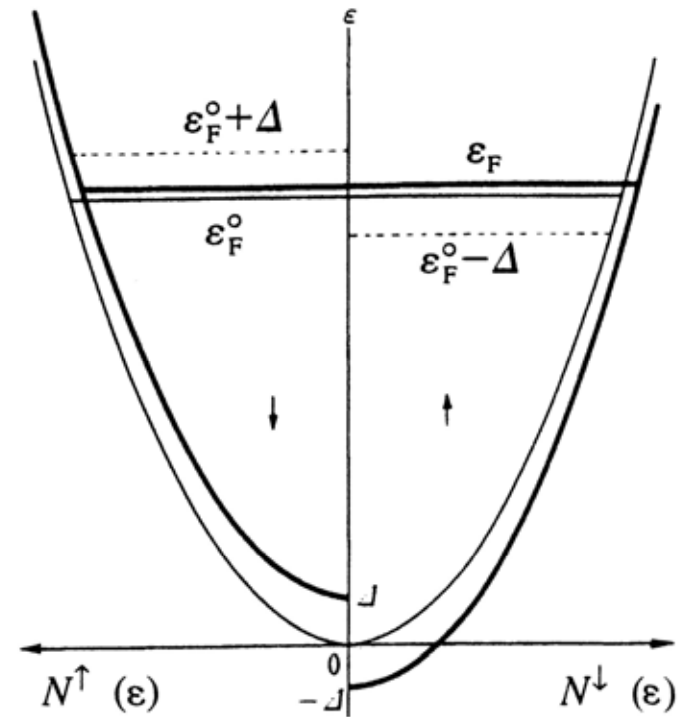
□ O-mediated super-exchange coupling between adjacent Mn spins favors **antiferromagnetism** .

□ Mediation by itinerant or delocalized empty majority-spin states in the vicinity of E_F favors **ferromagnetism**.

O-mediated super-exchange coupling

Mn   O   Mn
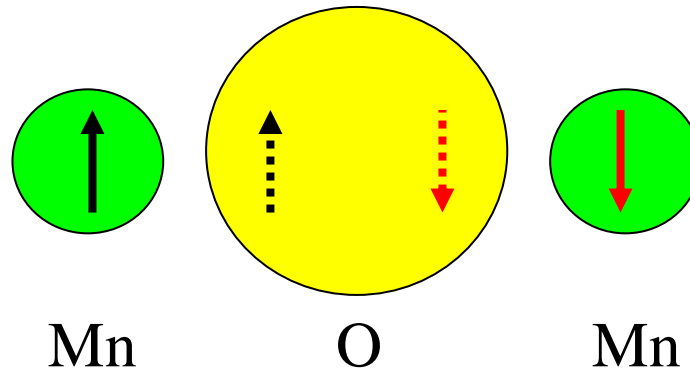
❑ For the **perovskite** structure, two adjacent Mn spins are separated by the O ion.
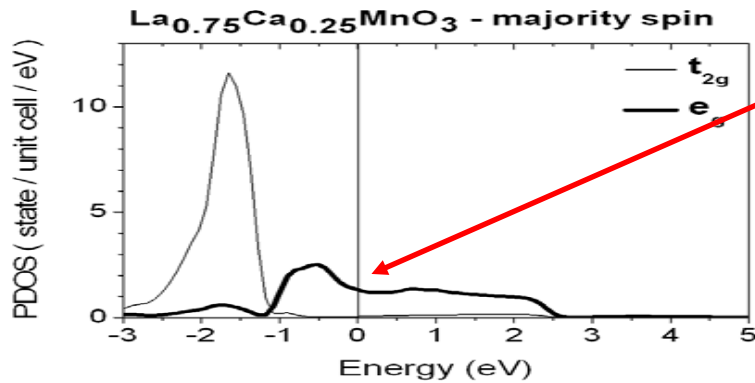
❑   -spin and   -spin electrons in the O ion can shift in opposite directions to benefit from **attractive exchange couplings** with the two opposite spins in the two neighboring Mn ions.

➡ Antiferromagnetism

Mediation by itinerant or delocalized empty majority-spin states in the vicinity of E_F

La$_{0.75}$Ca$_{0.25}$MnO$_3$ - majority spin

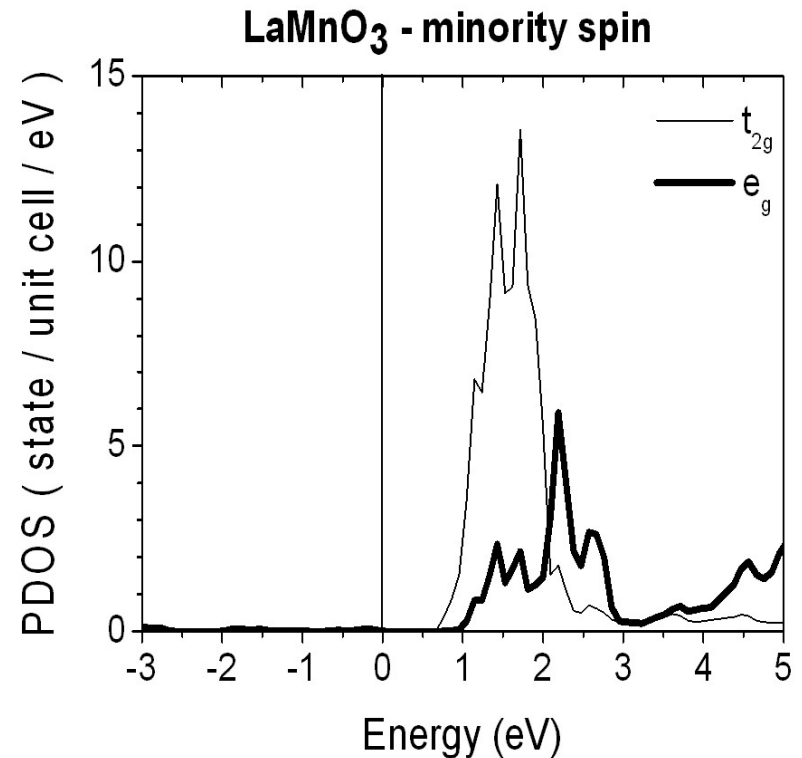La$_{0.75}$Ca$_{0.25}$MnO$_3$ - minority spin

delocalized Mn majority-spin empty e_g sub-band
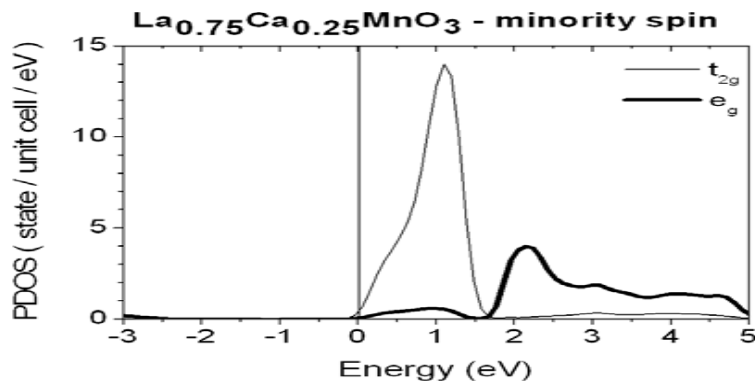
❑ Parallel spins have attractive exchange energy.

❑ The exchange energies between delocalized Mn majority-spin e_g electrons and neighboring localized Mn majority-spin t_{2g} electron are attractive.
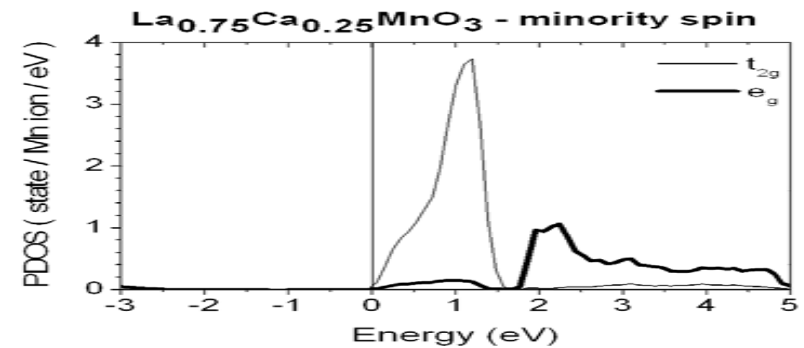
Ferromagnetism

The deficiency of Mn majority-spin e_g states immediately above E_F, so that the O mediated super-exchange coupling dominates and the material is **antiferromagnetic**.

Delocalized Mn majority-spin e_g

$La_{0.75}Ca_{0.25}MnO_3$

$La_{0.75}Ca_{0.25}MnO_3$ - majority spin

$La_{0.75}Ca_{0.25}MnO_3$ - minority spin
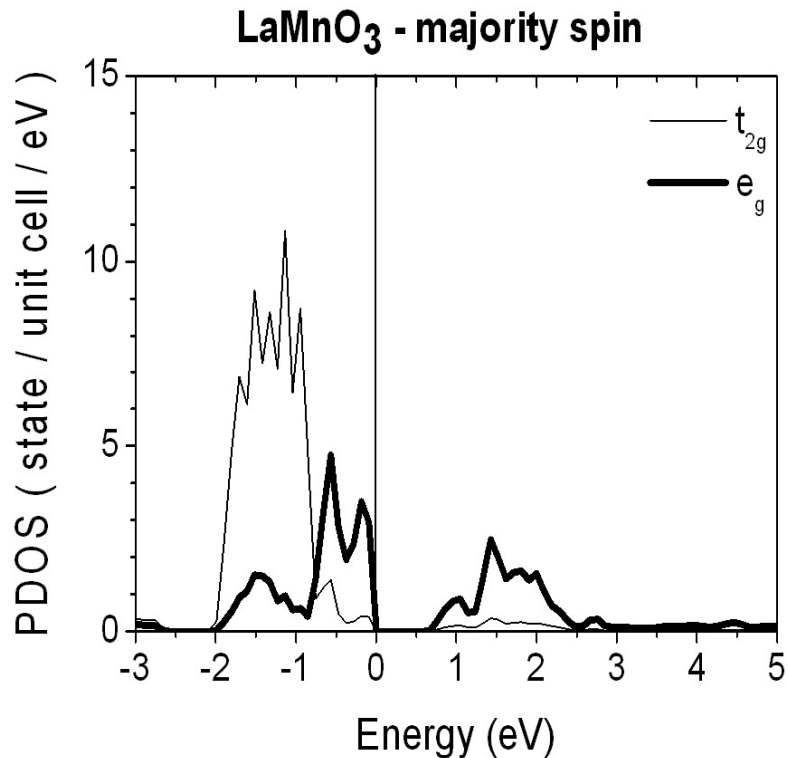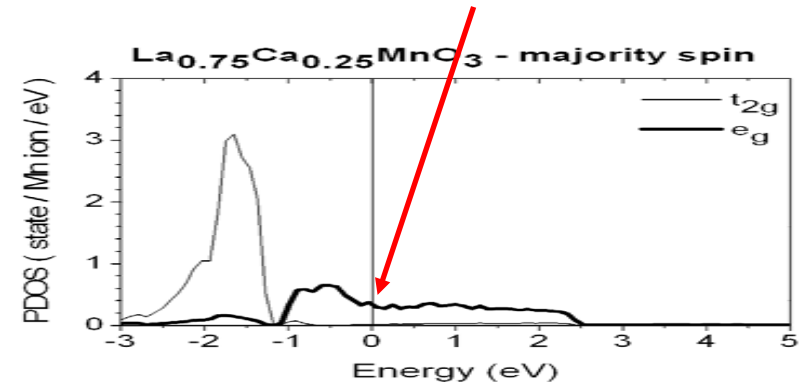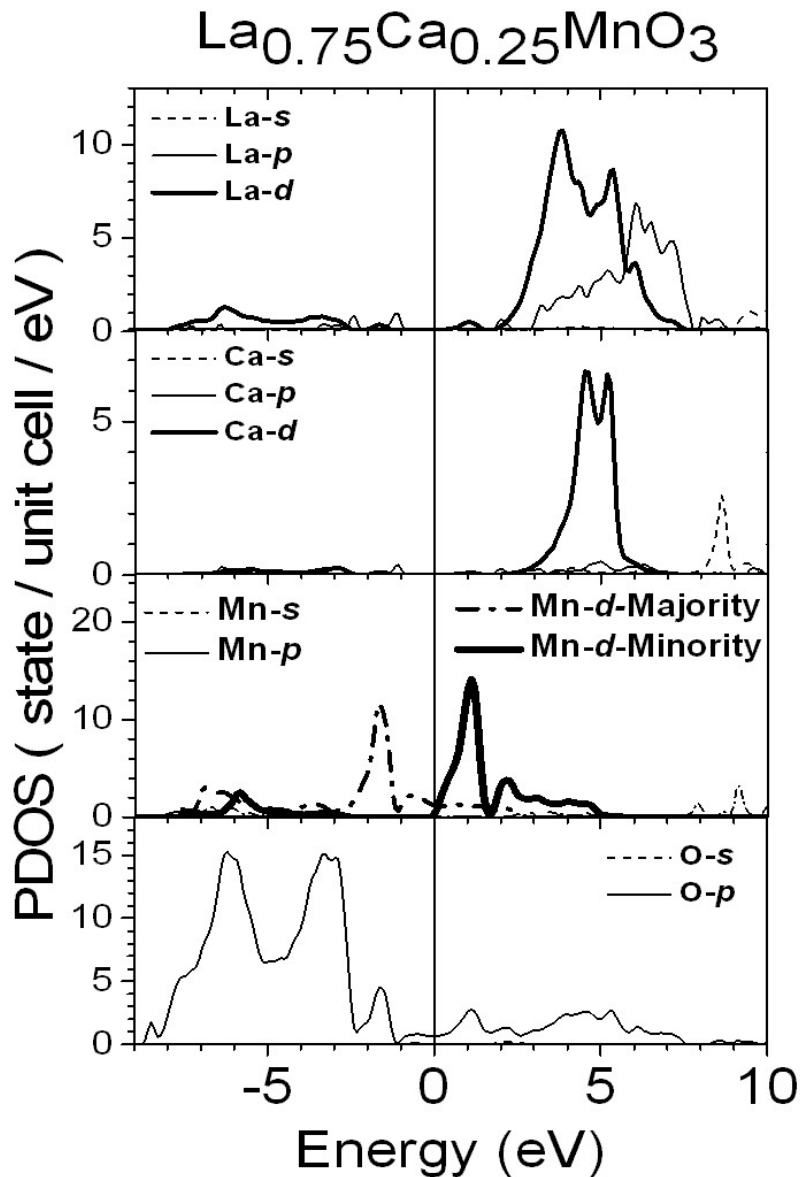
The delocalized empty Mn majority-spin e_g states immediately above E_F enhance delocalized-state mediated Mn-Mn spin couplings.

➡ Ferromagnetic

Delocalized Mn majority-spin e_g

La$_{0.25}$Sr$_{0.75}$MnO$_3$

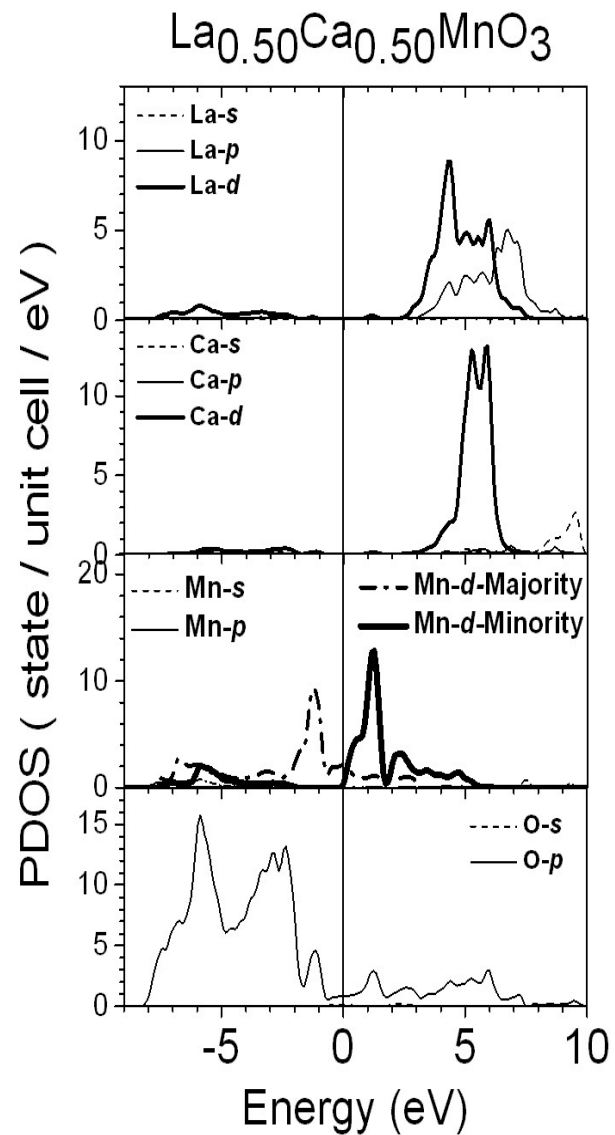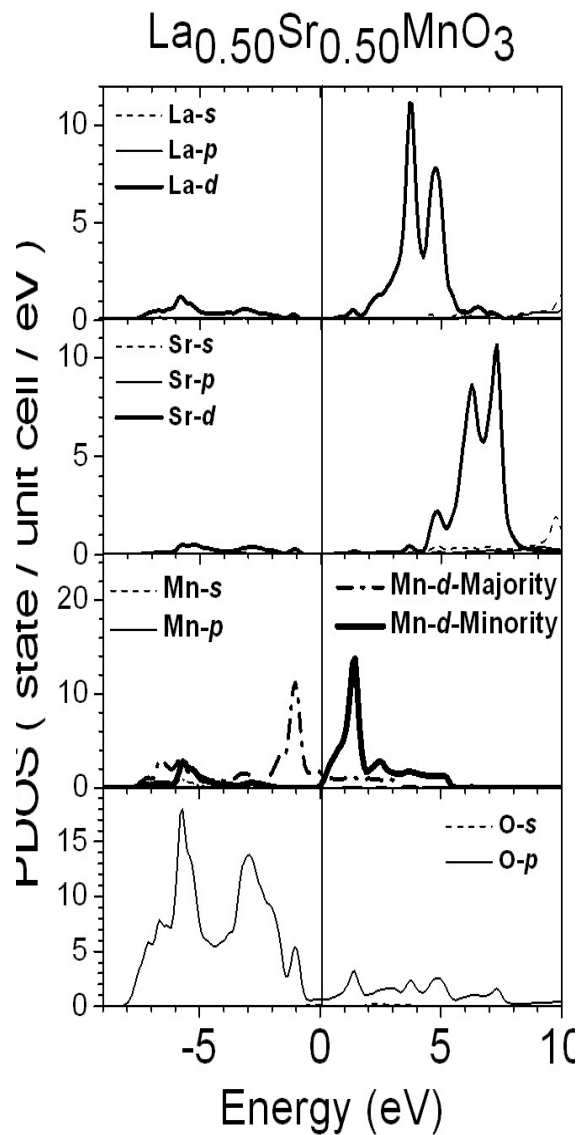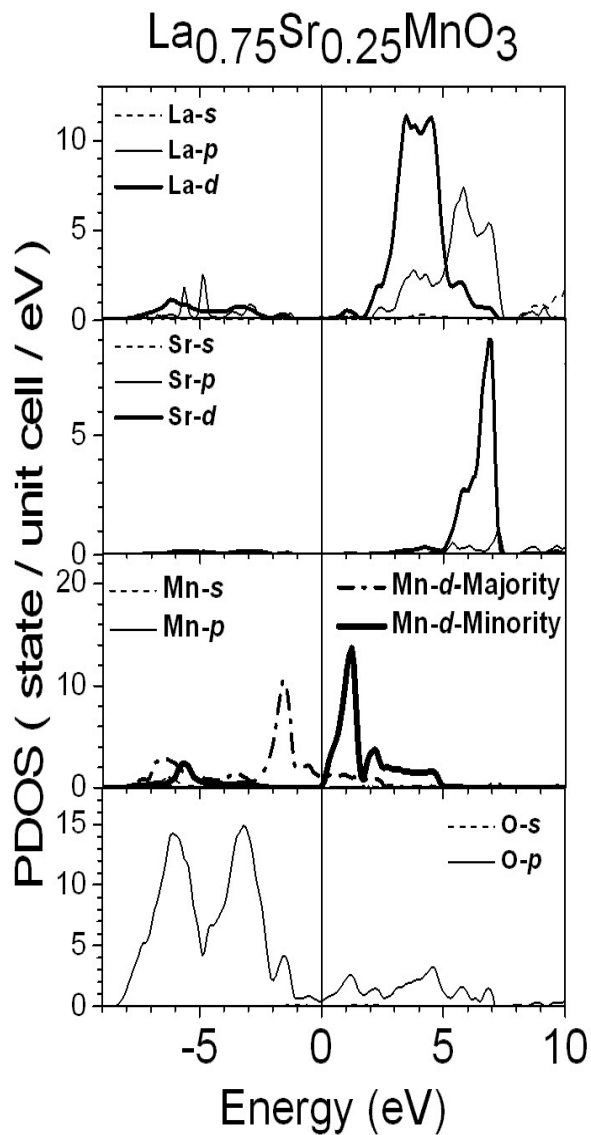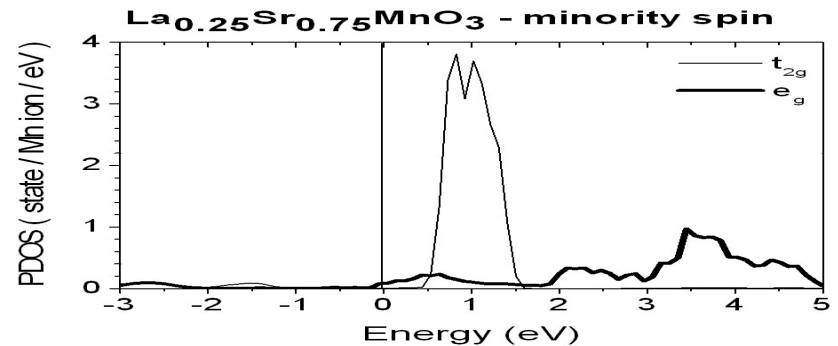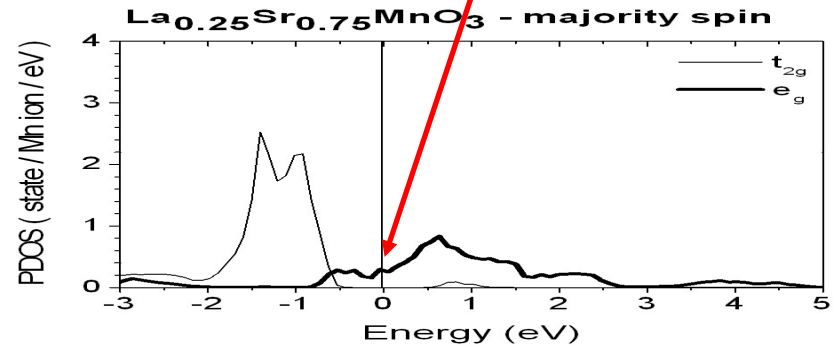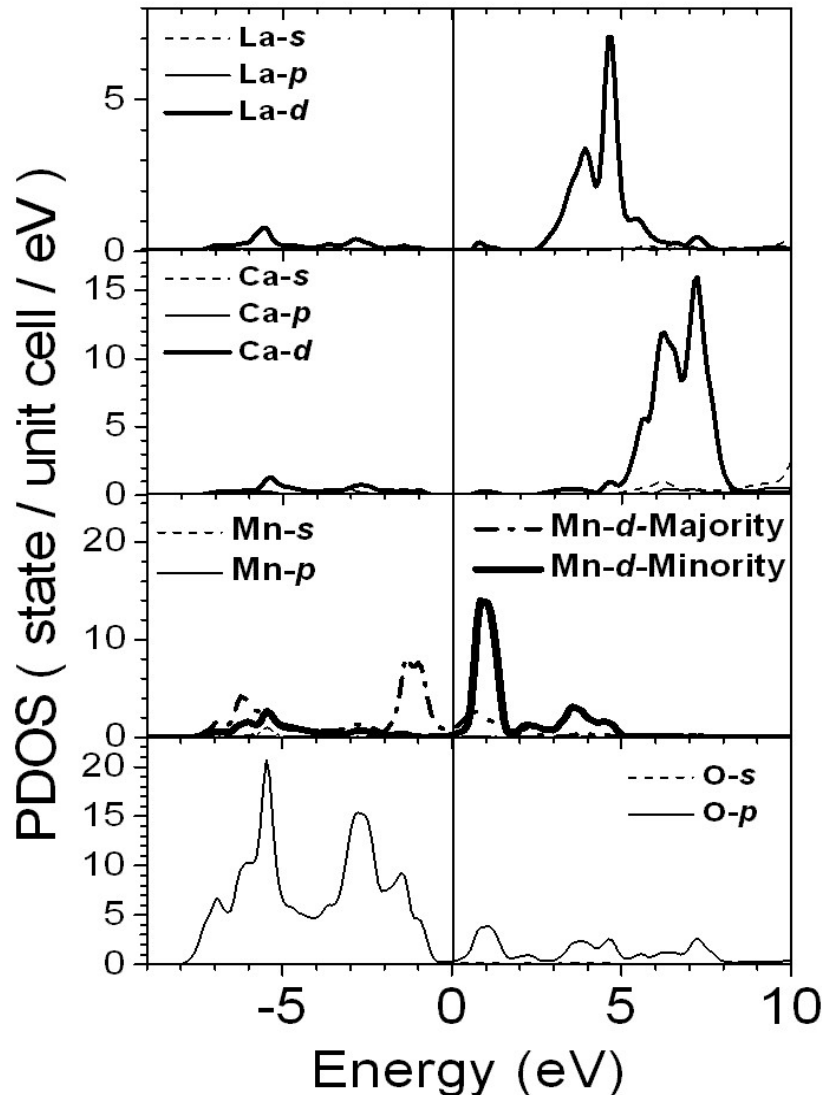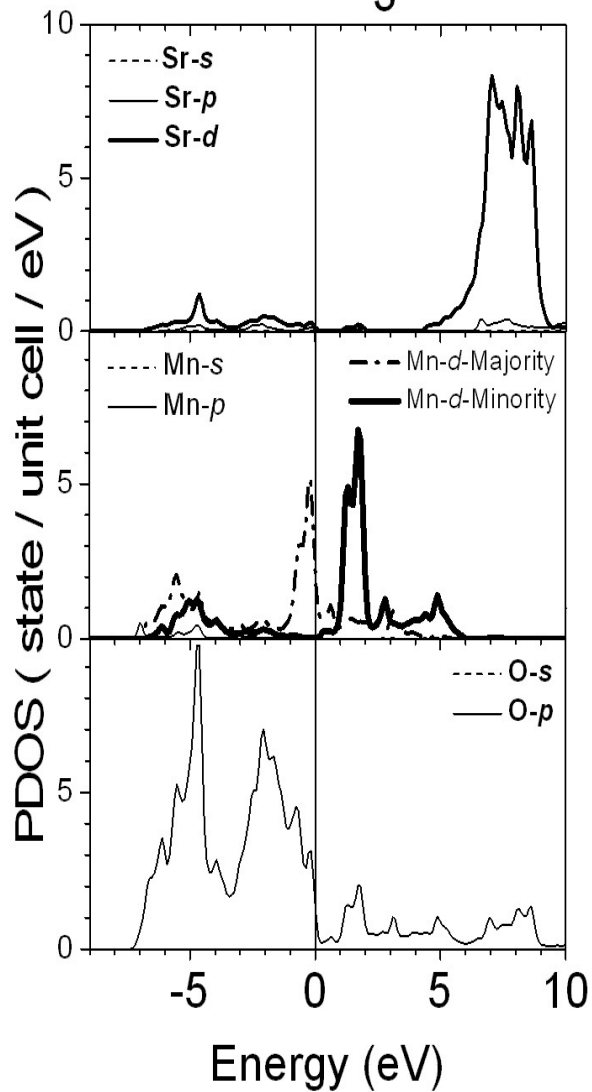Mn majority-spin e_g states trough region immediately above E$_F$ is reduced, which reduces delocalized-state mediated Mn-Mn spin couplings.
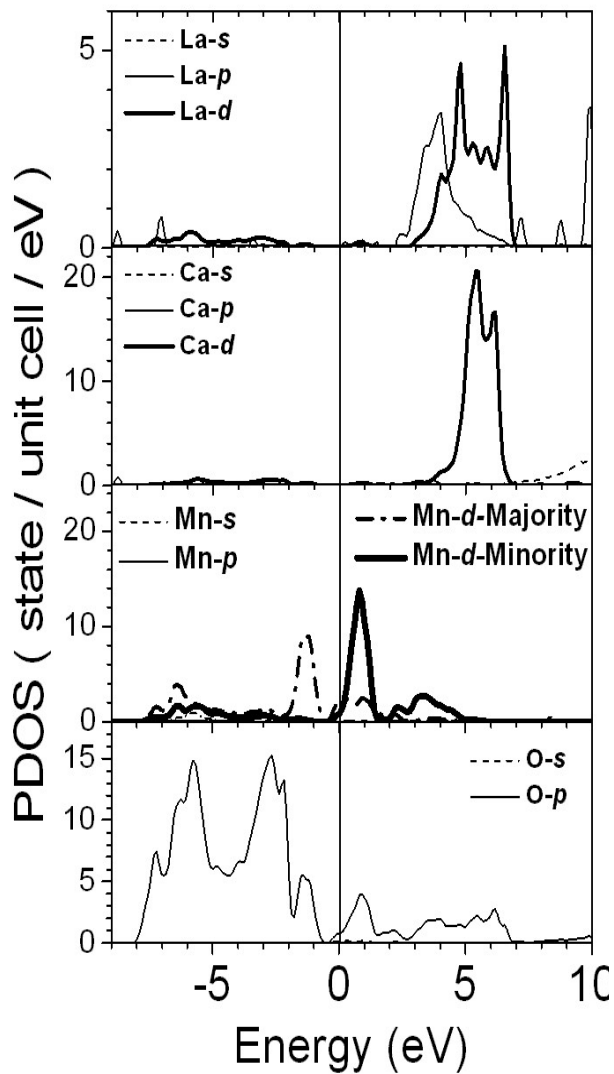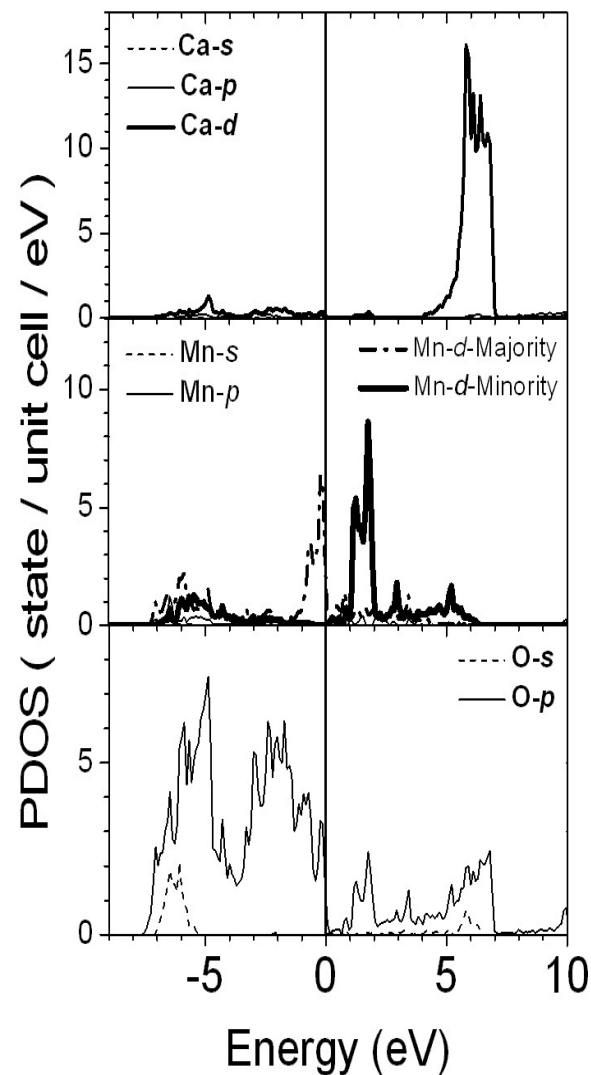
Antiferromagnetic

Implication to CMR

For doped manganites, there are three kinds of carriers: **(a)** delocalized O 2p electrons, **(b)** delocalized Mn e_g electrons and **(c)** localized Mn t_{2g} electrons. **(a)** and **(b) contribute dominantly to σ.**

(1) Without a magnetic field, $\rho=1/\sigma$ can be due to transfer of **(a)&(b)-**carrier energies to **empty** Mn t_{2g} states **immediately above E_F** through exchange interactions.

(2) Under a magnetic field strength of 6 Tesla:

ΔE(spin-field)=3.5×10^{-4}eV and ΔE(orbital-field)=$m3.5 \times 10^{-4}$eV (m=-2,-1,0,1,2) are **too small** to cause significant changes in **carrier densities** because **(a) and (b) sub-bands are not delta-function like.**

However, these ΔE's can cause a large percentage of reduction of the number of empty Mn t_{2g} states, which contribute to the absorption of (a)&(b)-carrier energies, due to the large slope of PDOS.

Note: ΔE(absorbed) per unit volume=$j^2\rho$, where j is the current density.

MR derivation is underway.

Electronic structures of wide-band-gap $(SiC)_{1-x}(AlN)_x$ semiconductors

- Between SiC and AlN :

  Small lattice mismatch & Large band gap difference

- Quaternary $(SiC)_{1-x}(AlN)_x$:

  Potential materials for opto-electronic applications.

  The wavelength of the light emitted can be tuned over a wide

  range.

- **MD method** is first used to efficiently obtain the structural parameters, and then the **PSF method** is used to obtain electronic structures, in particular band gaps.
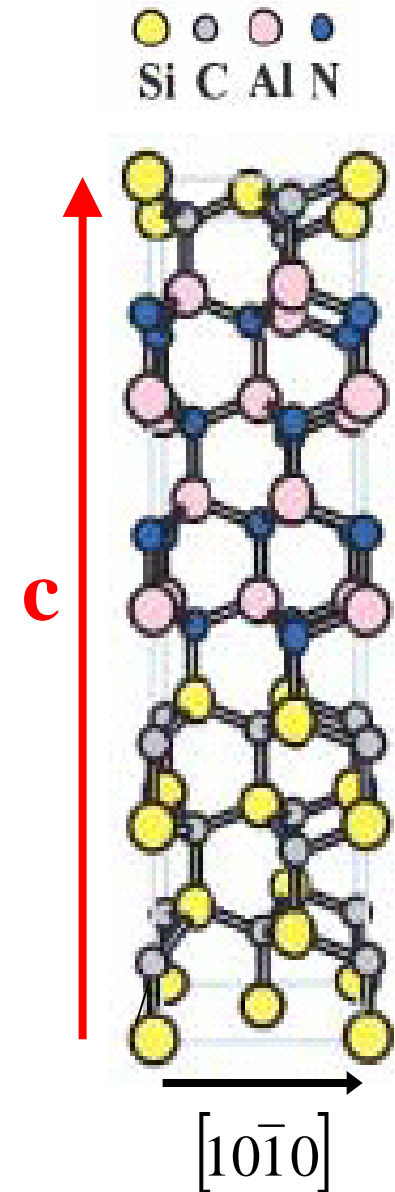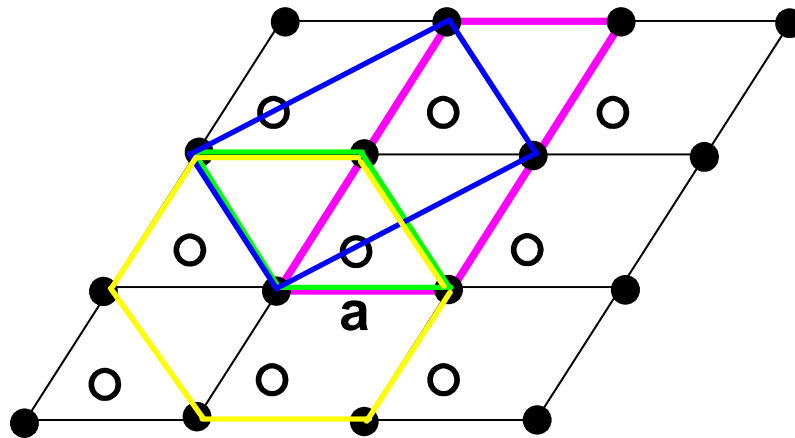
□ The $(SiC)_{1-x}(AlN)_x$ superlattice has been successfully fabricated on the 6H SiC(0001) substrate. [Roucka et al. PRL v.88 p.206102 (2002)]

□ x=0.00 (SiC) and 1.00 (AlN) :

Wurtzite primary unit cell with 4 atoms/cell

□ x=0.25, 0.50, and 0.75 :

$(2a,a,c)$ unit cell with 32 atoms/cell


Si C Al N

c

$[10\bar{1}0]$

Structural properties of $(SiC)_{1-x}(AlN)_x$

| x	0.00	0.25	0.50	0.75	1.00
a(Å)	3.02 (3.076 [1])	3.04	3.06	3.09	3.11 (3.110 [1])
c(Å)	4.91 (5.045 [1])	19.60	19.54	19.48	4.86 (4.980 [1])
u	0.360 (0.375 [1])				0.394 (0.382 [1])

❑ In the calculations of the electronic structures using the PSF method, the experimental lattice parameters of SiC and AlN are used, and the atomic positions are determined by prorating those optimized by MD calculations with experimental lattice parameters.

[1] F. Kootstra et al., Phys. Rev. B. **62**, 7071 (2000)

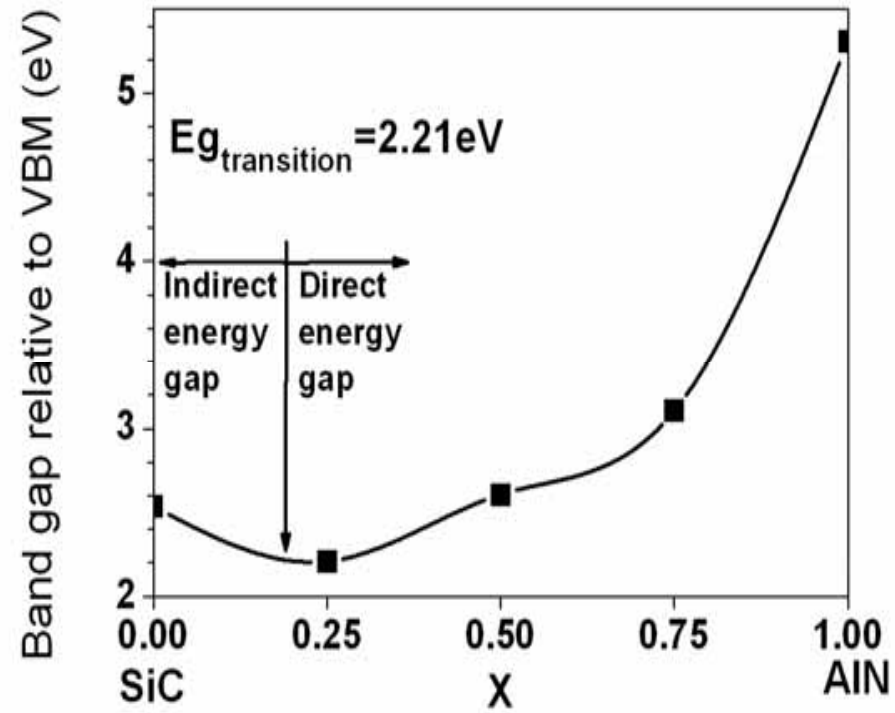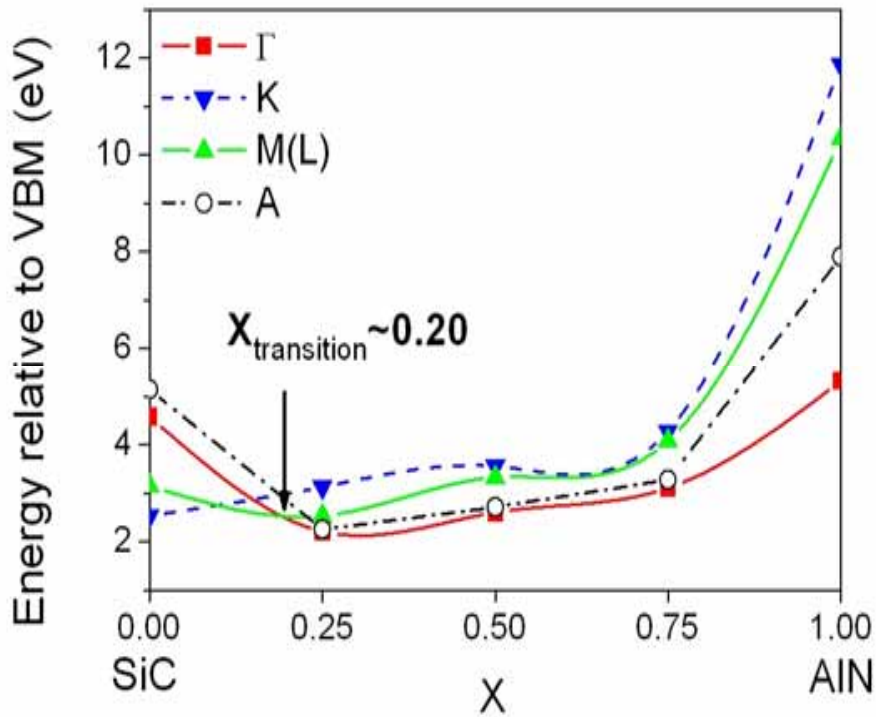# The band structures for $(SiC)_{1-x}(AlN)_x$

SiC (x=0.00)
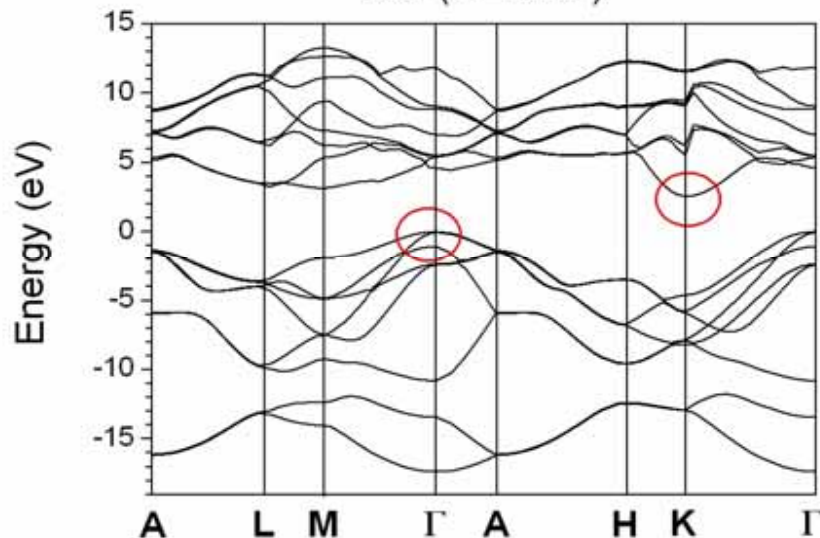
AlN (x=1.00)
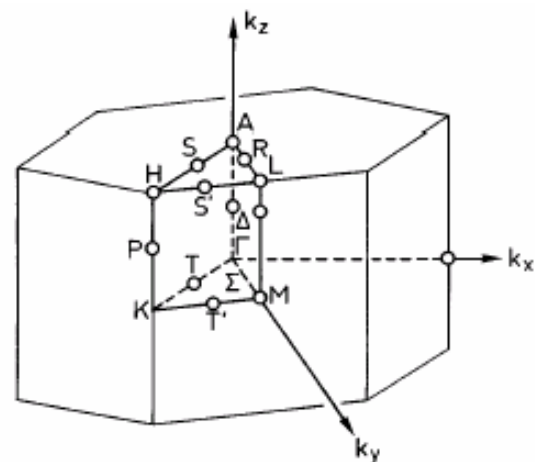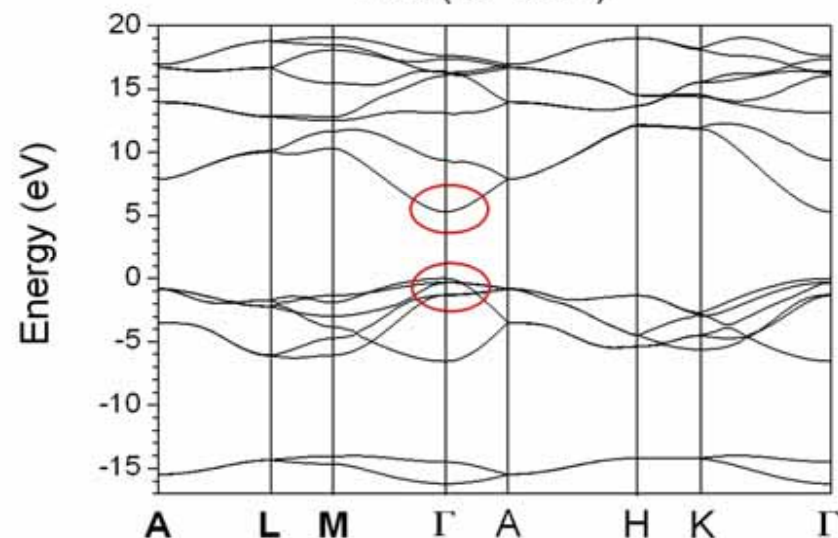
Indirect Band Gap
K

Direct Band Gap

Experimental band gap :

SiC : 3.33eV   AlN : 6.28eV

Direct band gap : 2.97 ~ 6.28eV

Light emission can be tuned
over a wide range of 3.31eV.

Conclusion

- Electronic structures of titanates, manganites, and $(SiC)_{1-x}(AlN)_x$ quaternary compounds are more complicated than those would be predicted from constituent binary or ternary compounds.

- Subtle charge transfer is found for these three kinds of quaternary compounds due to differing electronegativities and electronic configurations of cations and the detailed balancing in the filling of various sub-bands.

- The variation of the electronic and magnetic properties of Sr and Ca doped manganites is found due to both dopant-induced delocalization of -spin Mn e_g states and the lowering of the -spin Mn t_{2g} sub-band down to the Fermi-level.

- $(SiC)_{1-x}(AlN)_x$ is found to be important for optoelectronic applications.